Fall 2020

Feasibility study on novel fire-resistant coating materials

Anyou Zhu

Department:

FEASIBILITY STUDY ON NOVEL FIRE-RESISTANT COATING MATERIALS

by

ANYOU ZHU

A THESIS

Presented to the Graduate Faculty of the

MISSOURI UNIVERSITY OF SCIENCE AND TECHNOLOGY

In Partial Fulfillment of the Requirements for the Degree

MASTER OF SCIENCE IN CIVIL ENGINEERING

2020

Approved by:

Jenny Liu, Advisor
Hongyan Ma
Xiong Zhang

ABSTRACT

Over the past decades, wildfires in the United States have caused severe damage and property losses. The California Camp Fire in November 2018 caused 85 civilian fatalities and destroyed 18,793 structures. There is a need to enhance the fire resistance of structures and buildings. The primary purpose of this study was to develop innovative surface-bonded fire-resistant material that can be used as a wall coating with three primary features: (a) workability for application, (b) enough adhesion to the surface of the structure, (c) fire-resistant. This research developed mix designs of innovative fire-resistant coating materials including high-performance cement mortar (HPCM), geopolymer mortar (GPM), and magnesium phosphate (MPCM). And the then the feasibility of HPCM, GPM, and MPCM as fire-resistant coats for structures were investigated. The Taguchi method was used for the proportional design and material optimization of these materials. Then, a variety of performance tests relevant to the fire resistance of the potential fire-resistant coating materials (i.e., HPCM, GPM, and MPCM) were further conducted. The feasibility and potential for these materials as fire-resistant coatings were analyzed and discussed in detail. The present study results show that these developed materials had excellent slip resistance, cohesiveness, and adhesiveness as coating materials. They all had heat insulation to delay the heat transfer into the protected structures for 30 to 40 minutes. The results indicated that the fire-resistant performance of MPCM was better than HPCM and GPM, MPCM had better integrity after heating to 1000℃.

ACKNOWLEDGEMENTS

First, I would like to thank my advisor, Dr. Jenny Liu, for her extraordinary support. She gave me great ideas, expert advice, and encouragement whenever I needed guidance with research, beginning in Fairbanks when I took her properties of materials course and lasting throughout my graduate studies here in Rolla. I would also like to thank Drs. Hongyan Ma and Xiong Zhang for serving on my committee and providing timely feedback and support throughout my study.

A special shout-out to Hanli Wu for helping me with the experiments and revising my thesis. Thank you also to Yanping Zhu, who helped with the fire-resistant property test, and Alejandro Chavez, who helped me with the experiments. Thank you also to Mike Lusher, Jason Cox, and John Bullock for their help in the lab. I would also like to acknowledge the Center for Infrastructure Engineering Studies (CIES)'s assistance and support during the laboratory tests.

Lastly, I would like to thank my family and friends.

TABLE OF CONTENTS

Page

LIST OF FIGURES

LIST OF TABLES

1. INTRODUCTION

1.1. PROBLEM STATEMENT

Fire remains a severe risk to most structures and buildings around the world. Over the past decade, wildfires in the United States have caused more damage and property losses than ever before because more houses are being built on picturesque hillsides, in beautiful mountainous regions, and in other areas prone to wildfire. According to the U.S. Fire Administration (2019), it is estimated that 1,318,500 fires occurred in 2018, which resulted in 3,655 civilian fire fatalities, 15,200 civilian fire injuries, and approximately $25.6 billion in losses. On average, every 2 hours and 24 minutes, there was a civilian death caused by fire in 2018 (Evarts, 2019). New materials, designs, and construction techniques are needed to improve the fire-resistance of wood structures. One of the strategies is to use fire-resistant coating material to protect structures. Fire-resistant coatings that help structures from damage by fire have shown a growth over past ten years. This type of fire protection can slow the spread of flames, or delay a structural frame's fire-induced weakening. It can provide additional time to evacuate the occupants to safety from the fire threat. Conventional fire-resistant coating materials are divided into two broad categories: intumescent coatings and non-intumescent coatings. When intumescent fire-resistant coatings are heated, their volume can expand more than 10 times, and they generate an ash-like char layer that prevents the fire from spreading. The fire resistance of intumescent materials is excellent (Zhang et al., 2013). However, there are some shortcomings of the intumescent coatings. Firstly, ultraviolet exposure, operational heat, and humidity significantly affect the intumescent coatings. Secondly,

currently used intumescent coatings have some potential toxicity to humans. They are not suitable for places where people are living. Additionally, currently used intumescent coatings are relatively expensive when compared to non-intumescent coatings. Non-intumescent coatings can provide an inorganic ceramic barrier, which can slow down the transmission of heat, oxygen, mass, and volatile products (Qiu et al., 2018). However, currently used non-intumescent fire-resistant coatings that are designed for steel and plastics are not recommended for buildings or structures.

Conventional Portland cement concrete is virtually non-combustible because the components of Portland cement concrete (aggregates and Portland cement) are chemically inert. However, it is vulnerable to a notable phenomenon called spalling, which causes a fast layer-by-layer loss of mortar cover, conceivably prompting the protected structure's exposure to fire (Feng et al. 2012). Moreover, in order to make conventional Portland cement concrete or mortar a coating material, it needs to meet construction criterion such as workability, setting time, compressive strength, slip resistance, cohesiveness, and adhesiveness. Some emerging materials and technologies have shown great potentials for improvement in workability and fire-resistant performance (Abbas et al., 2016). Some examples include geopolymer and magnesium phosphate cement. Geopolymer is an inorganic material that can tolerate high temperatures and does not emit toxic fumes in high temperatures (Kong et al., 2008; Pan et al., 2009). Geopolymer also keeps a good structural integrity even after exposure to high temperature and has very little explosive spalling (Vickers, 2015). Magnesium phosphate cement is another possible fire-resistant coating material which is derived from reactions between phosphate and magnesium oxide (Yang et al., 2014). In 1970,

magnesium phosphate cement was developed as a rapid repair material in civil engineering (Seehra et al., 1993). Magnesium phosphate cement is quick setting and has high early-age strength (Park et al., 2016). It also has favorable bonding strength with old concrete and has excellent fire resistance (Hall et al., 2016; Fang et al., 2018), making magnesium phosphate cement a potential fire-resistant coating material. Moreover, magnesium phosphate cement demonstrates favorable durability compared with Portland cement (Yang et al., 2014). Nguyen also claimed that magnesium phosphate cement's heat resistance is quite stable in high temperatures up to 1020°C furnace temperature (Nguyen et al., 2012). Studies on geopolymer and magnesium phosphate cement for coating applications need to be explored.

In this study, the workability, early-age strength, and setting time were evaluated in an initial screening using the Taguchi Method to determine the mix proportion parameters of high-performance cement mortar (HPCM), geopolymer mortar (GPM), and magnesium phosphate cement mortar (MPCM) for coating application. A variety of performance tests relevant to the fire resistance of these materials were further conducted. The results were compared and discussed, from which conclusions and recommendations were made.

1.2. OBJECTIVE

The objective of this study is to develop mix designs of innovative fire-resistant coating materials including HPCM, GPM, and MPCM; then explore the feasibility of using three types of innovative materials as fire-resistant coating materials for structures.

1.3. RESEARCH METHODOLOGY

The following major tasks were completed to meet the objective of this study:

- Task 1: Literature review
- Task 2: Screening test and analysis
- Task 3: Performance tests of HPCM, GPM, and MPCM
- Task 4: Conclusion and recommendations

1.3.1. Task 1: Literature Review. A comprehensive literature review was conducted to collect information on key subjects related to this study, including research on application of intumescent and non-intumescent coating for fire protection, alternative materials such as Portland cement-based coating, geopolymer based coating and magnesium phosphate coating materials. This task is presented in Section 2.

1.3.2. Task 2: Screening Test and Analysis. Mortar samples of HPCM, GPM, and MPCM were prepared. To find the optimum mix design with good compressive strengths, workability, and setting time simultaneously, the Taguchi Method was used for experiment design. First, the influence factor was determined. The water/cement ratio, superplasticizer, accelerator, and viscosity-enhancing admixture contents were taken into account. For each factor, three levels were selected. Then, orthogonal arrays were used to specify which level combinations were to be used. All the mixtures designed by orthogonal arrays were tested.

After all the tests in orthogonal arrays were finished, the results were analyzed, and the optimum mix designs were determined by using Minitab. Then, a verification test was conducted. Finally, the modified optimum mix design was further investigated. This task is presented in Section 3.

1.3.3. Task 3: Performance Tests of HPCM, GPM, and MPCM. HPCM, combined with GPM and MPCM, were tested regarding their fire-resistant performance. The feasibility and potential of these three materials as fire-resistant coatings were analyzed and discussed in detail. Results were compared and discussed. This task is presented in Section 4.

1.3.4. Task 4: Conclusion and Recommendations. A summary was provided including the literature review, results from the screening tests, the optimization process for determining the optimum mixture designs, and performance results comparing the different materials determined through the analysis. The future areas of research were recommended. This task is presented in Section 5.

2. LITERATURE REVIEW

A comprehensive literature review was conducted, and the results and findings are summarized in this section. Applications of literature regarding current fire-protective coatings were presented. Development, application, and limitations of intumescent and non-intumescent coating for fire protection were reviewed. Special attention was given to conventional Portland cement-based fire-resistant coating materials and innovative coating materials, such as geopolymer and magnesium phosphate cement-based coating.

2.1. BACKGROUND

In the United States, nature fire has caused safety threats and enormous losses, including economic loss and environmental pollution. Fire is one of the most severe conditions to which structures may be subjected (Kodur, 2014). Structural fire damage causes thousands of deaths, injuries, and millions in property damage throughout the world each year (Brushlinsky et al., 2007). According to the Centre of Fire Statistics Data, there are approximately 510,000 structural fires reported each year, which means once every 62 seconds, a structural fire is burning somewhere in the world.

As more and more massive structural fires reported, fire hazards have got more and more attention. New construction methods are needed to improve the fire-resistant of new materials. Coating with fire-resistant materials is one of the strategies. This type of fire protection can slow the spread of fire, reduce its ability to penetrate an assembly, or delay a fire-induced weakening of a structural frame. It will provide increased

opportunity for people to escape from the buildings and provide enough time for the fire sprinklers and firefighting personnel to actively control the fire.

An effective coating has low toxicity, and high environmental compatibility. Fire-resistant coatings are cementitious coatings such as Portland cement, geopolymer, and magnesium phosphate cement based materials. With supplementary binders and some additives, advanced surface-bonding fire-resistant materials have potential. They can provide an excellent fire resistance, cost-effectiveness, weather resistance, enough adhesion, and good workability. This review emphasized cement-based surface-bonding materials. Their advantages and disadvantages were compared.

2.2. FIRE-PROTECTIVE AND FLAME-RETARDANT COATINGS

Fire-protective and flame-retardant coatings help structures from damage by fire. This type of fire protection can slow the flame spread, reduce its ability to penetrate an assembly, or delay a structural frame's fire-induced weakening. The conventional fire-resistant coating materials are mainly divided into two broad categories: intumescent coatings and non-intumescent coatings. They have been widely used as commercial coatings, however, both of them had some limitations, such as vulnerable to the environment, toxicity, and high cost.

2.2.1. Intumescent Fire-resistant Coatings. Intumescent fire-resistant coatings work by expanding their volume over 10 times and generating an ash-like char layer that slow the fire exposure. Expansion then occurs again, and the number of times the process repeats itself depends upon the coating's thickness. The shape of the structure usually affects the expansion and char formation (Zhang et al., 2013).

Conventional fire-resistant coating materials are divided into two broad categories: intumescent coatings and non-intumescent coatings. When intumescent fire-resistant coatings are heated, their volume can expand more than 10 times, and they generate an ash-like char layer that prevents the fire from spreading. The fire resistance of intumescent materials is excellent (Zhang et al., 2013). However, there are some shortcomings of the intumescent coatings.

Vandersall (1971) presented the early history and the development of commercial intumescent coatings, mostly based on a char-forming carbonaceous material, a mineral acid catalyst, a blowing agent, and a binder resin. The intumescent coating swells to a thick insulating foam to protect the wall when heated above a critical temperature. Different fire-resistant material have different fire protective mechanisms. Nitrogen-containing fire-resistant material can absorb heat and produce noncombustible gases to dilute the concentration of combustibles during polymers' decomposition process (Xing et al., 2011). Silicone-containing fire-resistant material often form an insulating layer on the polymer surfaces upon burning, thereby effectively impeding the transmission of oxygen, heat, and mass and reducing polymers' flammability (Alongi et al., 2015). Much empirical research has been done in the industry to optimize intumescent coatings and to find alternative char-formers, catalysts, blowing agents, optimized binders, activators, and residual barrier-forming additives. Even conventional paints, as some non-intumescent coatings, can reduce flame spread more than an unpainted flammable substrate. Intumescent and non-intumescent coatings have been successfully used for building structure coating, especially steel and wood. However, there are challenges. Firstly, ultraviolet exposure, operational heat, and humidity of the work area are three

major factors that affect the intumescent's performance. Intumescent materials are particularly vulnerable to environmental exposure at the time of application. Secondly, they have some potential toxicity to humans and the environment. Lastly, it is not cost-effective to use intumescent coatings. This is why highly effective and environmentally benign flame retardant materials are attracting increasing attention.

2.2.2. Non-intumescent Fire-resistant Coatings. Generally, non-intumescent coatings mainly consist of inorganic nanoparticles, which can be divided into zero-dimensional assembly, one-dimensional assembly, and two-dimensional assembly according to their sizes. The non-intumescent coating can provide an inorganic ceramic barrier, effectively hindering the transmission of heat, oxygen, mass, and volatile products (Alongi et al., 2014).

One type of non-intumescent fire-resistant coatings is silicone. Silicone coatings with dispersed carbon nanotubes were introduced as Nanocyl's ThermoCyl to give fire protection to a wide variety of substrates, such as plastics, cables, textiles, foams, metals, and wood. Coatings as thin as 100 mm have been shown effective.

A German research institute developed a fire-protective coating for wood based on criticizing sodium borate and silica compositions. Coatings such as Al_2O_3–TiO_2, ZrO_2, and other ceramic thermal barrier coatings are used to protect structures with short-term exposure to high temperatures. Ceramicizable compositions, suitable for cable coatings and seals, were developed by an Australian group based on a silicone polymer, mica, and a combination of low melting glass and high melting glass. When the organic component has burned away, these inorganic materials can form a self-supportive ceramic coating in the high temperature (Hamdani et al., 2009).

2.3. ALTERNATIVE MATERIALS

Some other materials such as cement, geopolymer, and magnesium phosphate cement are proved to be inert to fire. These materials have potential to be fire-resistant coating materials.

2.3.1. Portland Cement-based Coating. Portland cement mortar has been widely used as coating material for steel pipes and steel rebar. It exhibits protective properties on underground steel pipes, such as corrosion inhibiting properties, self-sealing effects, and increased insulation resistance with the aging of the line (Unz, 1960). Cement mortar-based coating also showed an anti-corrosion potential on steel rebar (Tang et al., 2013). However, limited research has been done on using cement-based material as a fire-resistant coating. It is a possible coating material if the mixture has required workability, slip resistance, cohesiveness, and adhesiveness to be able to apply onto the structural surface.

Portland cement concrete generally provides the best fire resistant property when compared to other construction materials such as steel and timber. This fire resistance is due to concrete constituent materials such as cement and aggregate. When it is heated, it is essentially inert and has low thermal conductivity, high heat capacity, and slower strength degradation with temperature increasing. This slow rate of heat transfer and strength loss enables concrete to act as an effective fire shield. It protects adjacent spaces and itself from fire damage (Kodur, 2014).

Concrete has been used as a fire resistance material widely. Nonetheless, concrete’s strength and durability properties are altogether affected when exposed to high temperatures because of chemical and physical changes (Crozier et al., 1999). When the

temperature is higher than 300°C, evaporation of the bound water makes the concrete weakening and causes compressive strength decreasing. At the point when temperatures above 400°C, calcium silica hydrates (C–S–H) go through degradation. The greater part of the original strength is lost somewhere in the range of 600 and 800°C (Koksal et al., 2012). Further, in fire conditions, concrete is vulnerable to a notable phenomenon called spalling, which causes a fast layer-by-layer loss of mortar cover, conceivably prompting the protected structure's exposure to fire (Feng et al., 2012). Dangerous spalling may have a serious ecological effect. Bits of crushed concrete can fly with high speeds and explosive energy, causing losses (Ali et al., 2001). For instance, a fire that happened in the Channel Tunnel caused a major loss in 1996 due to the spalling of concrete, and a repair cost of $1.5 million per day (Ulm et al., 1999).

2.3.2. Geopolymer Based Coating. An alternative coating material that possesses fire-resistant property is a geopolymer. A geopolymer is synthesized from a two-part mix, consisting of an alkaline solution and solid aluminosilicate materials (Feng et al., 2012). It is produced by the chemical action of inorganic molecules using none of the Portland cement, but fly ash. Fly ash is a by-product of coal obtained from the thermal power plant. It contains silica and alumina. When it reacts with an alkaline solution, it produces aluminosilicate gel that can act as the concrete's binding material. Geopolymer has high compressive strength, high-temperature stability, low thermal conductivity, and high thermal engineering applications (Lyon, 1997). Geopolymers can be widely used as an alternative construction material to the existing plain cement concrete. It can be used to fireproof building materials, sound heat insulators, and encapsulate hazardous waste (Dimas et al., 2009).

Regarding fire resistance, when compared to Portland cement-based systems, geopolymer retains a significant structural stability level after exposure to fire and shows just minimal spalling (Yang et al. 2014). The lesser explosive spalling in geopolymers is attributed to the large numbers of interconnected small pores. The enormous quantities of interconnected little pores accelerate the departure of moisture when heated, which makes geopolymer less damaged (Van Riessen et al., 2009).

Shaikh et al. (2014) asserted that as a result of the thermal incompatibility between coarse aggregates and geopolymer paste, the compressive strength of geopolymer diminished at raised temperatures up to 400 °C, which is consistent with Portland cement concrete. Nevertheless, the geopolymer showed higher compressive strength at 600 and 800 °C because of the generally stable geopolymer contraction at those temperature ranges. After introduction to elevated temperatures at 800 °C, the strength of the geopolymer still increased. It is because there are some un-reacted fly ash particles (Kong et al., 2007). However, at temperatures from 400 to 600 °C, Portland cement strength decreased more than geopolymer. The loss of moisture inside Portland cement leads the reduction of strength (van Riessen et al., 2009).

Generally, the fly ash-based geopolymer concrete has better fire resistance. It shows no spalling. It also has better thermal stability at high temperatures, less mass loss, smaller expansion ratio, and lower thermal conductivity than Portland cement concrete (He et al., 2020). However, very limited research has been done on investigating fire-resistant properties of geopolymer-based material as a coating. Giancaspro et al. (2006) applied a thin coating of a geopolymer containing glass microspheres to balsa wood sandwich panels to act as a fire-resistant barrier. Only 1.8 mm thick coating met the

Federal Aviation Administration (FAA) requirements for both heat release and smoke generation. Further investigation is required to explore the fire-resistant properties of geopolymer-based material as a coating.

Except having better fire-resistant properties than Portland cement concrete, geopolymer is also a more environmentally friendly material.

McLellan et al. (2011) announced that geopolymer has an expected 44–64% improvement in greenhouse gas emissions over Portland concrete. The expense of these geopolymers can be up to twice as high as Portland concrete. Nonetheless, he indicated that those advantages are only realizable, given the most suitable feedstock source and the least cost transportation. If a carbon tax of $20 / ton CO_2 is considered, most geopolymer feedstocks become cost-competitive. The production of 1.0 tone of geopolymer cement generates 0.180 tons of CO_2, from combustion carbon-fuel, compared with 1.00 ton of CO_2 for Portland cement (Davidovits, 2002). Geopolymer cement produces six times less CO_2 during manufacture than Portland cement (Davidovits, 2002). Likewise, energy consumption is determined to be around 60%, not as much as that needed by Portland concrete (Li et al., 2004).

2.3.3. Magnesium Phosphate Cement-based Coating. Magnesium phosphate cement (MPC) is phosphate-bonded inorganic material derived from phosphate and magnesium oxide reactions. It was first discovered and developed as dental cement in the late 19th century (Wilson and Nicholson, 2005). In 1970, MPC was developed as rapid repair materials in civil engineering (Seehra et al., 1993). During decades of development, MPCs have been employed in many fields, including stabilized and solidified and light MPC foamed material, rehabilitation of the structure, and 3D powder

printing materials (Yunsong, 2002; Klammert, 2010). MPC demonstrates favorable durability performance compared with Portland cement (Yang et al., 2014). Except for durability, MPC also possesses other advantages over HPC. Firstly, it has quick setting and hardening properties. Secondly, it has high early strength; rapid development of compressive strength can be achieved within several hours, and the strength can exceed 22.8MPa after 1 hour (Park et al., 2016). Thirdly, it has favorable bonding strength with old concrete (Hall et al., 1998). Lastly, it has fire-proof capabilities (Fang et al., 2018). These superior properties endow MPCs with the potential to be widely used in structures.

Fire-resistant properties for MPC are superior compare to Portland cement and geopolymer. Sugama and Kukacka (1983) reported that the strength kept rising as they heated MPC to 1300 °C. The stability of MPC at high temperatures is an important characteristic that makes MPC suitable for refractory applications. Some research-tested the fire-resistant property of MPC at elevated temperatures, which shows details about MPC performance at elevated temperatures. The strength of MPC specimens decreased significantly when the temperature passed 130 °C, then the strength of MPC decreased slowly when temperature continued to increase. The mass loss at 130 °C was maximum. When temperature passed 130°C, the rate of mass loss became smaller. The reason was that the crystal water inside $MKP{\cdot}6H_2O$ had mainly been lost in the prior stage at 130 °C, and the hydration products almost turned into $KMgPO_4$ (MKP) (Li et al., 2015). According to Thermal analysis, the heating temperature had less influence on MPC when the temperature surpassed 200 °C. Lastly, at 1000 °C, residual strength was about 30% (Li et al., 2015). Nguyen et al. (2012) also claimed that MPC's heat resistance is stable in contact with high temperatures up to 1020°C in the furnace; the fire retardation

throughout the 30mm thickness of this material is effective, it reached about 120°C after 2 hours, and it can be developed for fireproof application on structures. Gardner et al. (2015) also reported that above 1000°C, no cracking or spalling of the samples was observed, but there were additional crystalline phases and microstructural changes. These results indicate that MPC have excellent fire resistance and it can potentially become a fire-resistant coating material. However, there's very limited literature on using magnesium phosphate cement as coating material.

3. SCREENING TESTS AND ANALYSIS

In this study, innovative coating materials were developed for fire-resistant coatings. The screening tests of HPCM, GPM, and MPCM mortar were conducted to find the optimum mix design; the optimum mix design should have reasonable workability, setting time, and a reasonable compressive strength at the hardened stage. The Taguchi Design proposed by a Japanese engineer Genichi Taguchi (Ranjit et al., 2001) was adopted in this study. The method utilizes two-, three-, and mixed-level fractional factorial designs. Several factors were taken into consideration when making mixtures. For example, different water/cement, superplasticizer/cement, and viscosity-modifying admixture (VMA) /cement ratios were considered as the factors that affected HPCM's workability, setting time, and compressive strength. Laboratory tests were conducted to find the optimum mixtures. For optimization of mixtures, a fractional factorial design based on an orthogonal array was used to evaluate the effects of various key factors on both the fresh and hardened properties of HPCM, GPM, and MPCM. Then the properties of the optimum mixture were verified; the optimum mixture was then used for further performance testing.

3.1. MATERIALS AND SPECIMEN PREPARATION

Materials including HPCM, GPM, and MPCM were prepared. Screening test mixtures were made using different levels of different ingredients. Specimens were mixed and fabricated using ASTM standards.

3.1.1. HPCM. The materials, mixtures preparation, mixing method, and specimen fabrication of HPCM were discussed in this part.

3.1.1.1. Materials. The conventional Portland cement mortar components include water, cement, sand, and admixtures, like superplasticizer, air-entraining agents, retarders, accelerators, silica fume, and fibers. Different from the conventional Portland cement mortar, the HPCM developed in this study has unique workability, quick setting speed, and adequate compressive strength. The HPCM coating mortar must have good workability to be to apply on the surface of a building structure. Setting quickly allows it to adhere on vertical surfaces. Lastly, it should be strong enough. An accelerator mixture makes the mortar condense sooner and tick to the sliding. Thus, the amount of accelerator admixtures should be controlled and determined by the trial mixtures. The VMA is needed to get good rheological properties. Based on practical experience, high workability may result in poor stability of concrete. Thus, bleeding and segregation may occur in this mixture. VMA has been used to increase viscosity to solve this problem.

The materials used for the screening tests were aggregate materials, cementitious materials, and chemical admixtures, including accelerator and VMA. The aggregate used in the initial screening test was sand. Following ASTM C136, multiple sieve analyses were performed and gradation is presented in Figure 3.1. The fineness modulus of sand was 2.46. The cement used was type I cement. Class F fly ash was used. Fly ash can make the mixture more cost-effective, reduce permeability, and get better workability and ultimate strength. Silica fume was also used to improve durability. In addition, one type of superplasticizer, one type of accelerator, and one type of VMA were used.

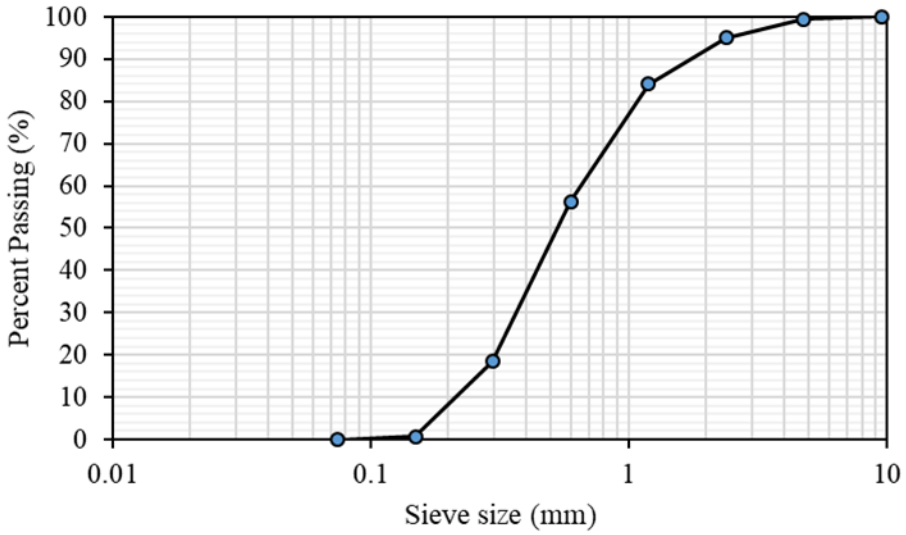

Figure 3.1 Aggregate gradation.

3.1.1.2. Mixture. A typical HPCM mortar comprises five main ingredients: water, sand, superplasticizer, accelerator, and VMA. In this study, fly ash, silica fume, and sand were not considered as influencing variables. A fixed ratio of 20% fly ash and 10% silica fume, based on the weight of cement, were used. The effect of the sand/binder ratio on the workability of the HPCM fresh mortar was observed during the trials. Too much sand tended to produce a harsh mixture with low workability and stiffness, causing difficulties in building surface application. However, mixtures containing a low proportion of sand were not cost-effective. A moderate sand/binder of 2.0 was adopted.

Four influencing variables on the properties of the HPCM mortar were taken into account, including water/binder, superplasticizer/binder, accelerator/binder and VMA/binder ratios. In the previous study, these variables were individually optimized to obtain good compressive strengths, workability, setting time, and viscosity.

In this study, the HPCM was optimally designed to obtain the best compressive strengths, workability, and setting time simultaneously by consideration of the four above variables. The Taguchi Method recommends five significant steps in the test design process. First, formulate the problem. Then, plan the experiment using orthogonal arrays. After that, analyze the results and confirm the improvement. Lastly, adopt the new design.

An orthogonal array has several rows and columns, each row is a test and each factor is in a column. Levels of each factor are shown in the tables. Using orthogonal arrays testing method, the number of factors was studied, and the number of levels for each factor was selected. For the water/cement ratio, three levels 0.32, 0.35, and 0.38 were selected. Three levels for superplasticizer, 10%, 15%, and 20% (weight % of binder), were defined. Initial trails provided the selection criterion. Also, to investigate the best HPCM setting time, three accelerator levels were considered: 0%, 2%, and 4%. Lastly, VMA contents were determined to be 0%, 0.14%, and 0.28%.

The influencing factors and their levels are listed in Table 3.1. There are 4 factors and 3 levels of each factor.

Table 3.1 Test Factors used and their levels.

Factors	Level 1	Level 2	Level 3
Water/binder	0.32	0.35	0.38
Superplasticizer/binder	0.7	1	1.3
Accelerator/binder	0	2	4
VMA/binder	0	0.14	0.28

Before selecting the orthogonal array, the minimum number of tested experiments needed to be fixed based on the total number of degrees of freedom. The minimum number of experiments required to study the factors had to be more than or equal to the total degrees of freedom available. The number of degrees of freedom associated with a factor is equal to one less than the number of levels for that factor (Antony et al., 2012). In this study, the number of degrees of freedom for all the factors was 9. An L9 orthogonal array satisfied this requirement. This array assumed that there is no interaction between any two factors. As a result, instead of all the possible states ($4^3 = 64$ tests), it was enough to test nine specimens with levels of each factor indicated in Table 3.2.

Table 3.2 Overall orthogonal array testing design.

Experiment No.	Water/ Binder	Superplasticizer/ binder	Accelerator/ binder	VMA/ binder
1	1	1	1	1
2	1	2	2	2
3	1	3	3	3
4	2	1	2	3
5	2	2	3	1
6	2	3	1	2
7	3	1	3	2
8	3	2	1	3
9	3	3	2	1

Note: The “1”, “2”, “3” stand for different levels from Table 3.1.

3.1.1.3. Mixing. The standard used for mixing was ASTM C305 – 14. First, the dry paddle and the dry bowl were placed in the mixing position in the mix. All the materials—including cement, sand, supplementary cementing materials, water, and

chemical admixtures—were measured using dry buckets. Then, the mortar container was pre-wetted before filling in with fresh mortar. The water and all the chemical admixtures were added into the bowl, then all the cement and supplementary cementing materials were added into the container on top of the liquids. The mixer was started at slow speed for the 30s, then the entire quantity of sand was slowly added over a 30 second timespan, period while mixing. Then, the mixer was stopped and changed to medium speed and mixed for 30 seconds. After that, the mixer was stopped, and the mortar stood for 90 seconds. Finally, it was mixed for 60 seconds at medium speed.

3.1.1.4. Specimen fabrications. After mixing, molds were filled according to ASTM C109/C109M - 16a. The total elapsed time was 2 min and 30 s, after completing the original mixing of the mortar batch and before molding the specimens. To begin, a layer of mortar was placed in all of the cube compartments, taking up approximately one half of the mold's depth and totally about 1 inch. The mortar in each cube was tamped 32 times in about 10 s taking 4 rounds. Then, the compartments with the remaining mortar were filled and tamped the same as the first layer. After tamping, excess cement was struck off, the mortar surface was then smoothed and covered. After 24 hours, samples were removed from their molds, labeled, and cured in the moisture room.

3.1.2. GPM. The materials, mixtures preparation, mixing method, and specimen fabrication of GPM were discussed in this part.

3.1.2.1. Materials. The Class F fly ash was used as the base material to make the GPM. The chemical and physical analyses including the mineral compositions of the fly ash are presented in Table 3.3.

Table 3.3 Chemical and physical analysis of the fly ash (*Photo courtesy of ENX*).

CHEMICAL ANALYSIS				
TEST DESCRIPTION	TEST RESULTS	UNITS	SPECIFICATION LIMITS	
			CLASS F	CLASS C
Silicon Dioxide (SiO_2)	59.70	%	-	-
Aluminum Oxide (Al_2O_3)	21.90	%	-	-
Iron Oxide (Fe_2O_3)	4.50	%	-	-
Total (SiO_2) + (Al_2O_3) + (Fe_2O_3)	86.10	%	50% (min)	50% (min)
Sulphur Trioxide (SO_3)	0.20	%	5.0% (max)	5.0% (max)
Calcium Oxide (CaO)	6.10	%	18.0% (max)	> 18.0%
Magnesium Oxide (MgO)	1.40	%	-	-
Moisture Content	0.35	%	3% (max)	3% (max)
Loss on Ignition (LOI)	1.34	%	6% (max)	6% (max)
Total Equivalent Alkali Content (Na_2Oeq)	-	%	-	-
Total Available Equivalent Alkali Content (Na_2Oeq)	0.81	%	-	-

PHYSICAL ANALYSIS				
TEST DESCRIPTION	TEST RESULTS	UNITS	SPECIFICATION LIMITS	
			CLASS F	CLASS C
Fineness Retained on 45µm (No. 325 Sieve)	22.2	%	34% (max)	34% (max)
Quantity of Air Entrainment	1.00	%	-	-
Drying Shrinkage (Increase at 28-days)	0.10	%	0.03% (max)	0.03% (max)
Strength Activity Index with Portland Cement				
% of Control at 7-Days	75	%	75% (min)	75% (min)
% of Control at 28-Days *(previous month's result)*	84	%	75% (min)	75% (min)
Water Requirement, Percent of Control	99	%	105% (max)	105% (max)
Soundness, Autoclave Expansion	0.01	%	0.8% (max)	0.8% (max)
Density	2.11	g/cm^3	-	-
Density, Variation from Average	0.00	%	5% (max)	5% (max)
Fineness Retained 45µm, Variation from Average	0.00	%	5% (max)	5% (max)

The alkaline activator used in this study was a combination of sodium hydroxide (NaOH) and sodium silicate (Na_2SiO_3). NaOH was used because it is inexpensive, and it is the most widely available alkaline hydroxide. Also, the hydroxyl ion in NaOH is an important element to start the geopolymerisation process (Provis and Van Deventer, 2009).

Sodium silicate (Na_2SiO_3) is a high viscosity chemical in liquid or powder form. It influences the GPM mixture workability when powder or liquid is added in high concentration. Na_2SiO_3 in the GPM system increases the paste's final strength and binds the material together to produce a dense paste (Jo et al., 2007).

NaOH and sodium silicate together creates the quickest setting time and advances the breakdown of both micropores and mesopores, along these lines increasing compressive strength (Jiang, 1997). Most of research stated that activation with sodium silicate blended with NaOH gets the most compressive strength (Zhao and Sanjayan, 2011; Nazari et al., 2011; Adam et al., 2010; Guo et al., 2010; Pimraksa et al., 2008). Thus, the mix of sodium silicate and sodium hydroxide as an alkaline activator was used.

The NaOH was in powder form with 99% purity. Water was added to make it a solution, and the compositions of the sodium silicate solution are shown in Table 3.4.

Table 3.4 Composition of sodium silicate solution.

SiO_2/Na_2O	sodium silicate/water	Wt. % Na_2O	Wt. % SiO_2	Density g/cm^3	Viscosity centipoise
3.22/1	37.5/62.5	8.90	28.7	1.39	180

3.1.2.2. Mixtures. In this research, the water/fly ash, fly ash/alkaline activator solution ratio, and Na_2SiO_3/ NaOH ratios were taken into account as the three influencing variables on the properties of the GPM mortar. By considering the three above variables, the GPM was optimally designed to have the best simultaneous compressive strengths, workability, and setting time.

Similar to the HPCM mortar analysis, the Taguchi method was used to reduce the number of tests. By using the orthogonal arrays testing method, the number of factors was studied, and the number of levels for each factor was selected.

Sathonsaowaphak et al. (2009 and 2012) revealed that the principle factors influencing fresh GPM mortar's workability were sodium silicate/hydroxide ratio and sodium hydroxide concentration. Higher sodium silicate/hydroxide ratio and sodium hydroxide concentration lead to less workable mortar because of higher viscosity of sodium silicate and sodium hydroxide.

Several factors can affect GPM mortar's compressive strength. Sukmak et al. (2013) considered the impact of sodium silicate/sodium hydroxide and alkaline activator solution/fly ash ratios on GPM's compressive strength. The outcomes indicated that ideal ratios for sodium silicate/sodium hydroxide and alkaline activator solution/fly ash were 0.7 and 0.6, individually. Ridtirud et al. (2011) detailed that GPM mortars with a sodium silicate/sodium hydroxide ratio of 1.5 yielded the highest compressive strength (45 MPa) contrasting with mortars made with lower sodium silicate/sodium hydroxide ratios. Some researchers also featured the requirement for proper adjustment of silicate/hydroxide ratios to improve GPM mortar's compressive strength (Sathonsaowaphak et al., 2009; Guo et al., 2010; Nazari et al., 2011).

Therefore, water/fly ash, fly ash/alkaline activator solution, and Na_2SiO_3/NaOH ratios were selected as three factors in the Taguchi design, and for each factor, three levels were used, as shown in Table 3.5.

Table 3.5 Test Factors used and their levels.

Factors	Level 1	Level 2	Level 3
Water/fly ash	0.25	0.28	0.31
Fly ash/alkaline activator solution	2.0	2.5	3.0
Na_2SiO_3/NaOH	2.0	2.5	3.0

The minimum number of experiments to be tested need to be fixed based on the total number of degrees of freedom. The standard orthogonal array chosen in this test was L9. Table 3.6 shows the overall orthogonal array testing design.

Table 3.6 Overall orthogonal array testing design.

Experiment No.	water/fly ash	Fly ash/alkaline	Na_2SiO_3/ NaOH
1	1	1	1
2	2	2	2
3	3	3	3
4	1	2	3
5	2	3	1
6	3	1	2
7	1	3	2
8	2	1	3
9	3	2	1

Note: The “1”, “2”, “3” stand for different levels from Table 3.5.

3.1.2.3. Mixing. The fly ash and the fine sand were first mixed in a mixer for about 3 minutes. The mixture’s liquid component was then added to the dry materials, and the mixing continued for about 4 minutes to fabricate the fresh mortar. The fresh mortar was cast into the molds immediately after mixing and compacted by vibrating the molds for 20 seconds on a vibrating table.

3.1.2.4. Specimen fabrications. After casting, the test specimens were covered with vacuum bagging film to minimize the water evaporation during curing. Curing was at room temperature. After the curing period, which was the first 24 hours, the test specimens were demolded and left to air-dry in the lab.

3.1.3. MPCM. The materials, mixtures preparation, mixing method, and specimen fabrication of MPCM were discussed in this part.

3.1.3.1. Materials. MPCM mortar was prepared using the dead burned magnesium oxide (MgO), potassium dihydrogen phosphate (KH_2PO_4), and sand. Borax ($Na_2B_4O_7 \cdot 10H_2O$) was used as a retarder.

3.1.3.2. Mixtures. The molar ratio of magnesium to phosphate were set at three different levels. Other detailed information of the test factors and their levels were presented in Table 3.7. Binder means the mixture of magnesia and phosphate. The ratios are all in mass.

Table 3.7 Test Factors used and their levels.

Factors	Level 1	Level 2	Level 3
Magnesium/phosphate (molar ratio)	6	8	10
Borax/binder	0	0.05	0.1
Water/binder	0.2	0.22	0.24

The minimum number of experiments to be tested needed to be fixed based on the total number of degrees of freedom. The standard orthogonal array chosen in this test was L9. Table 3.8 shows the overall orthogonal array testing design.

3.1.3.3. Mixing. Borax, phosphate, and water were poured into the mixer in sequence and mixed for 60s at low speed. The sand was then added and mixed for another 60s at low speed then 30s at high speed. After that, magnesia was added slowly

and mixed for 90s at low speed then paused for 30s, before mixing at high speed for 90s (Grantham et al. 2009). The fresh mortar was then cast into the molds immediately after mixing and compacted by vibrating the molds for 20 seconds on a vibrating table.

Table 3.8 Overall orthogonal array testing design.

Experiment No.	Magnesium/phosphate (molar ratio)	Borax/binder	Water/binder
1	1	1	1
2	1	2	2
3	1	3	3
4	2	1	3
5	2	2	1
6	2	3	2
7	3	1	2
8	3	2	3
9	3	3	1

Note: The “1”, “2”, “3” stand for different levels from Table 3.7.

3.1.3.4. Specimen fabrications. After casting, the test specimens were covered with vacuum bagging film to minimize the water evaporation during curing. The specimens were demolded after 30 minutes to 1 hour. They were cured in the lab at a temperature of 20 ± 1 °C and a relative humidity of 50 ± 5%. Compressive strength tests were carried out at 1, 2, and 24 hours.

3.2. TESTING PROCEDURES

All of the performance testing procedures used followed ASTM standards, unless noted otherwise.

3.2.1. Compressive Strength. For compressive strength, ASTM C109/C109M was followed. Specimens were crushed at a rate of 200 pounds per second. The samples were demolded 24 hours after mixing and then cured in a moisture room with 80% relative humidity at 23°C. The compressive strength was measured at 1 day, 3 days, and 7 days. (Figure 3.2). The compressive strengths recorded were the average of three replicates.

Figure 3.2 Compressive strength test setup

3.2.2. Workability. To measure workability, ASTM C230 was followed. The flow table test setup is shown in Figure 3.3. First, the flow table was wetted. Then, the cone was placed in the center of the flow table and filled with fresh mortar in two equal layers. Each layer was tamped 10 times with a tamping rod. A wait time of 30 seconds was implemented before lifting the cone. When the cone was lifted, the concrete was allowed to flow freely. The flow table was then lifted 40 mm and dropped 25 times,

causing the mortar to flow. Lastly, the maximum spread in two directions parallel to the table edges was measured as $F= (d_1+d_2)/2$.

Figure 3.3 Flow table test setup

3.2.3. Setting Time. The initial and final setting time for the mortar was determined according to ASTM C403 using penetration resistance measurements. The elapsed time after initial contact between cement and water that was required for the mortar to reach a penetration resistance of 500 psi (3.45 MPa) is defined as initial setting time, and the elapsed time to reach a penetration resistance of 4000 psi (27.58 MPa) is defined as final setting time. The setting time test set up is shown in Figure 3.4.

Figure 3.4 Setting time test set up.

3.3.RESULTS

The results of compressive strength, workability, and setting time for all 9 mixtures of HPCM, GPM and MPCM were collected.

3.3.1. HPCM. The results of compressive strength, workability, and setting time for the 9 mixtures of HPCM were discussed in this part.

3.3.1.1. Compressive strength. The 1-day, 3-day, and 7-day compressive strength results for 9 mixtures are reported in Figure 3.5. Mixture No.2 had the highest compressive strength. Mixtures No.1, No.2, No.3, and No.5 had the highest compressive strength at 1 day, 3 days, and 7 days. By comparing the water/cement ratios and the compressive strength of all the mixtures, mixtures No.1, No.2, and No.3 had the lowest water/cement ratio; it can be concluded that water/cement was the main factor for compressive strength. Since compressive strength could result from multiple factors, and these 9 mix designs had different levels of these factors, it was hard to determine which element was the dominant reason for compressive strength.

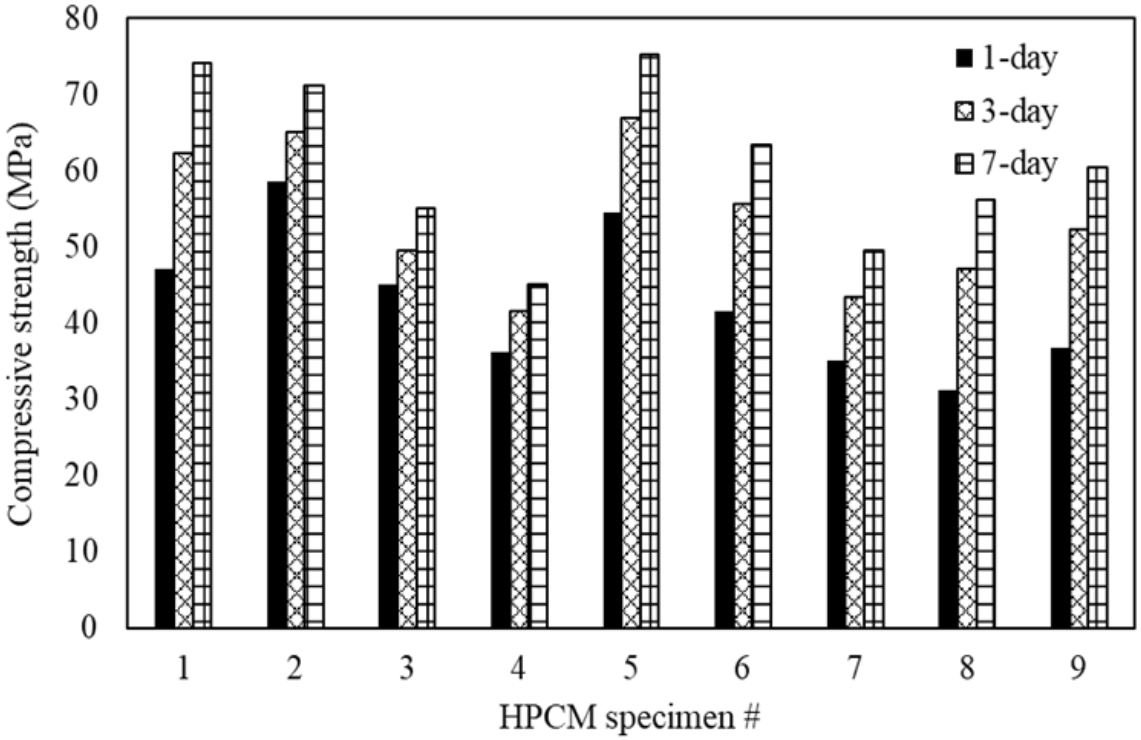

Figure 3.5 Compressive strength of each screening mixture for HPCM.

The analysis of how each factor affected compressive strength was discussed in the Minitab method. Figure 3.6 shows how each factor affected the compressive strength. It was found that increasing the cement ratio increased compressive strength. Increasing water decreased the 1-day compressive strength dramatically. Taking cement and water factors into consideration simultaneously, it can be found that when the water/cement ratio increases, the compressive strength also increased. The superplasticizer's content did not affect compressive strength. As VMA increased, the compressive strength decreased.

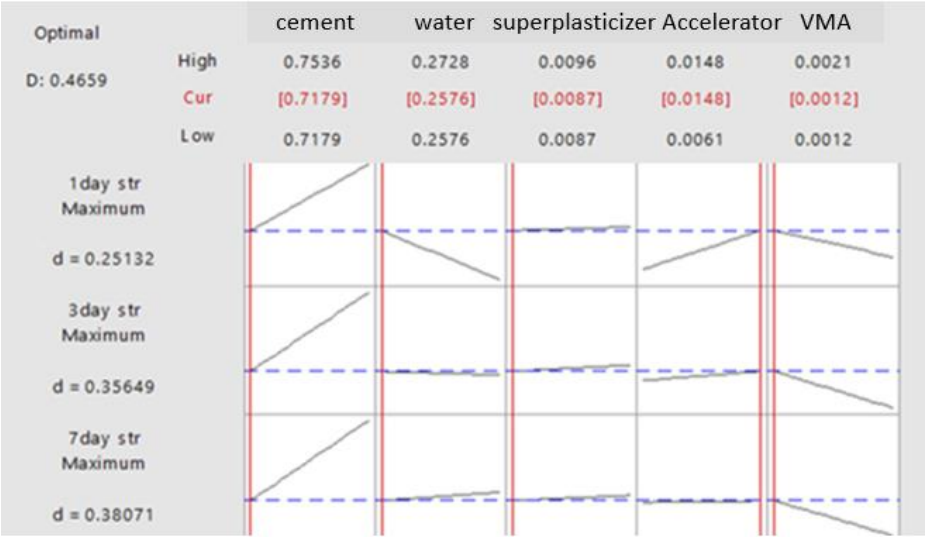

Figure 3.6 Factors affect compressive strength for HPCM.

3.3.1.2. Workability. Figure 3.7 shows the workability of the HPCM mortar. All the mortar mixes, except No. 5 and No. 9, showed relatively consistent behavior with flow table spread values within the range of 100 mm to 180 mm. Mixtures No.5 and No.9 flowed off the plate meaning they lacked enough viscosity. Therefore, 254 mm was used as the flow table spread value which was the plate's diameter for the test. No.5 and No.9 had high water/binder ratios. When doing the Minitab data analysis, the goal for the flow table test spread value was set from 160 to 230 mm. The results showed the higher the water/cement ratio, the greater the readings were. VMA also makes the flow table reading smaller. Comparing No.3 and No.1, No.3 had higher VMA content, yet water/cement ratios are the same. VMA may be the reason that makes mortar less workable.

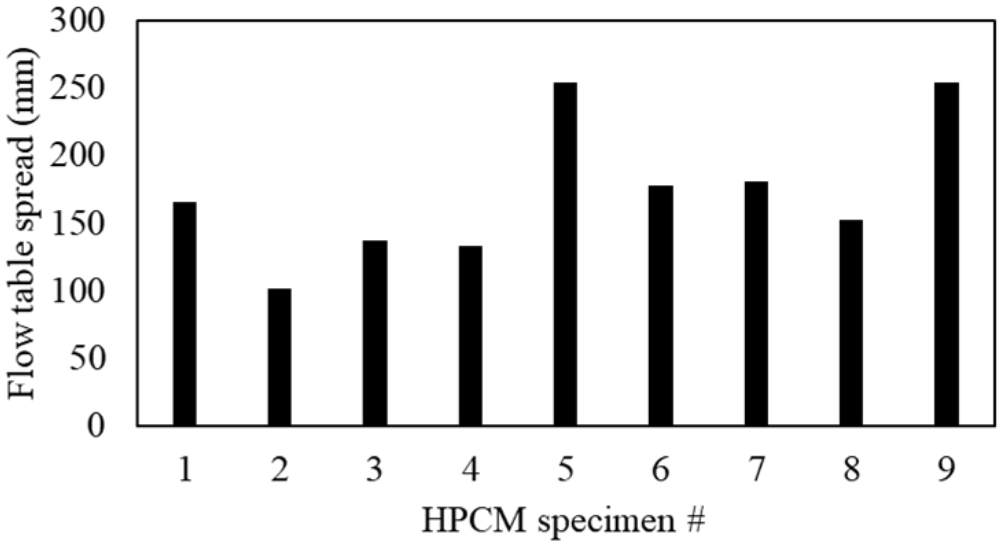

Figure 3.7 Flow table spread of each screening mixture for HPCM.

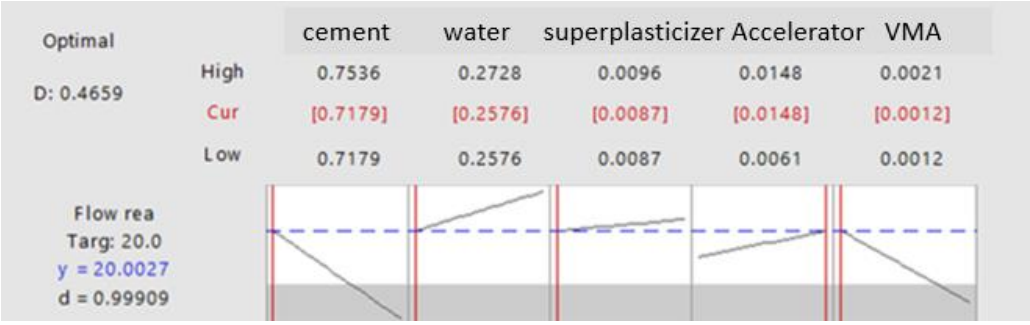

Figure 3.8 Factors affect the flow table spread results of HPCM.

As shown in Figure 3.8, the Minitab optimization plot gave more accurate results on how each factor affected the flow table results. As it shows, when the water/cement ratio increased, the flow table results got higher, which means the mortar had better workability. As superplasticizer and accelerator content increased, the mortar got slightly more workable, which can be ignored. However, increasing VMA content made the mortar less workable.

3.3.1.3. Setting time. Figure 3.9 shows mixtures No.3, No.5, and No.7 had the shortest setting times, and mixtures No.1, No.6, and No.8 had the relatively long setting time compare to other mixtures, which correlated with accelerator content very well. Mixtures No.3, No.5, and No.7 have the highest accelerator contents with 4% binder weight. However, mixtures No. 1, No.6, and No.8 had no accelerators. The ones with more accelerator (No.3, No.5 and No.7) had better setting time results for both the initial setting and final settings. The Minitab optimization plot in Figure 3.10 also shows the accelerator content as the dominant factor.

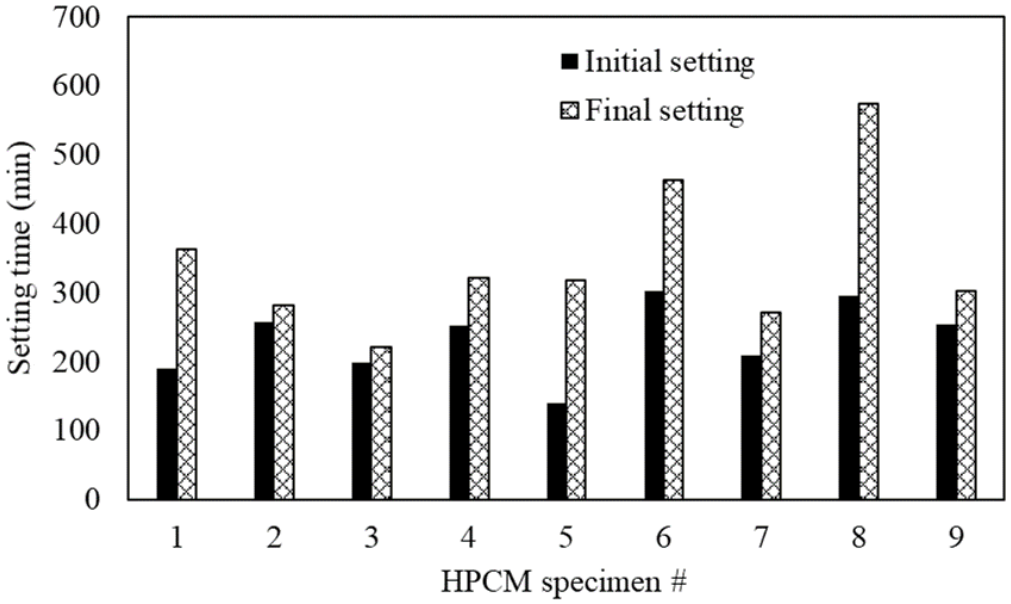

Figure 3.9 Initial and final setting time of each screening mixture for HPCM.

3.3.2. GPM. The results of compressive strength, workability, and setting time for the 9 mixtures of HPCM were discussed in this part.

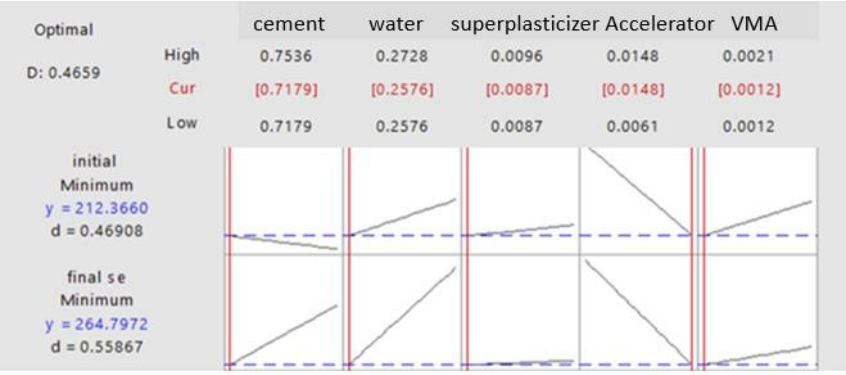

Figure 3.10 Factors affect setting time results for HPCM.

3.3.2.1. Compressive strength. As shown in Figure 3.11, mixture No.6 and No.7 had the highest 1-day compressive strengths. Pimraksa et al. (2011) reported that NaOH's concentration as an alkaline activator directly influences the strength of GPM. Higher concentration of alkaline activator molarity, representing higher Na_2O/Al_2O_3 and Na_2O/SiO_2 ratios caused the strength increasing. This correlates with the result from this study. As shown in Figure 3.12, when NaOH content increased, the strength increased**.**

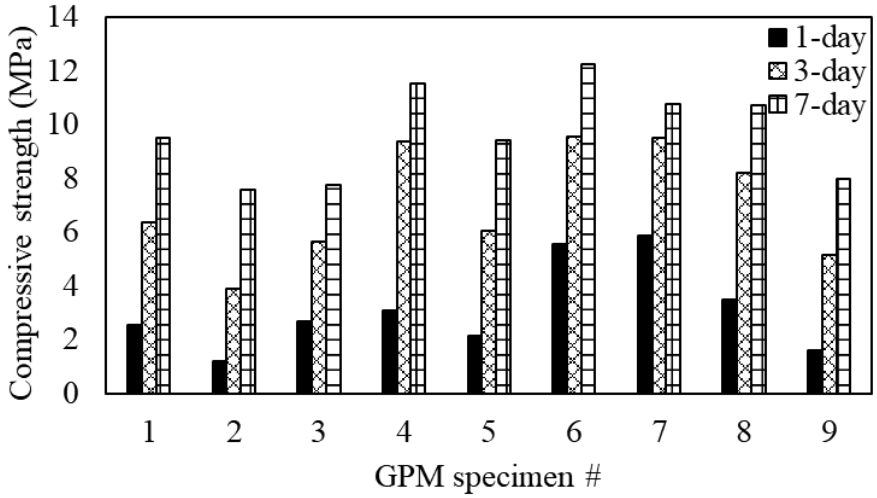

Figure 3.11 Compressive strength of each screening mixture for GPM

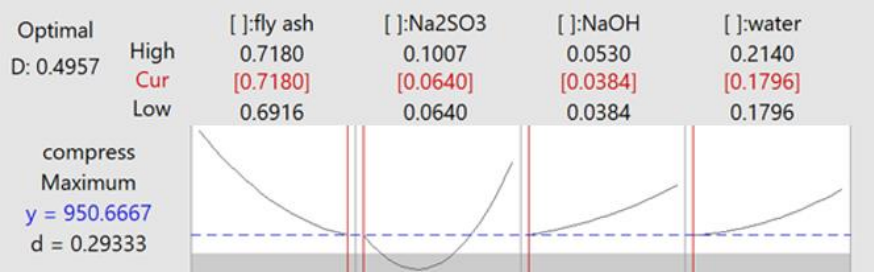

Figure 3.12 Factors affect compressive strength results for GPM

3.3.2.2. Workability. Figure 3.13 shows the workability of the GPM mortar. All the mortar mixes had flow table spread values within the range of 150 mm to 250 mm. Mixtures No.3, No.5 and No.9 had the spread value of 250 mm, and they flowed off the plate, meaning they lacked viscosity. Figure 3.14, from the Minitab optimization plot shows that when the water/fly ash ratio increased, the flow table results got higher, which means the mortar had better workability. However, Na_2SiO_3/NaOH ratios had a complex effect on flow table results. Saloma et al. (2017) reported that the lower usage of Na_2SiO_3 and NaOH ratios caused bigger slump flow diameter, which correlates with this study.

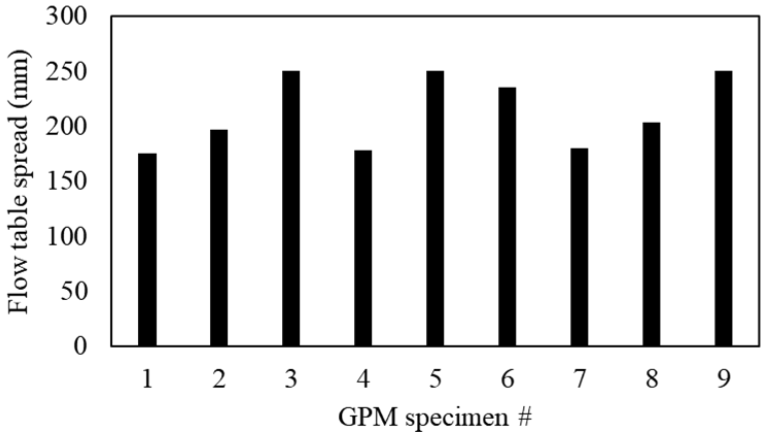

Figure 3.13 Flow table spread of each screening mixture for GPM.

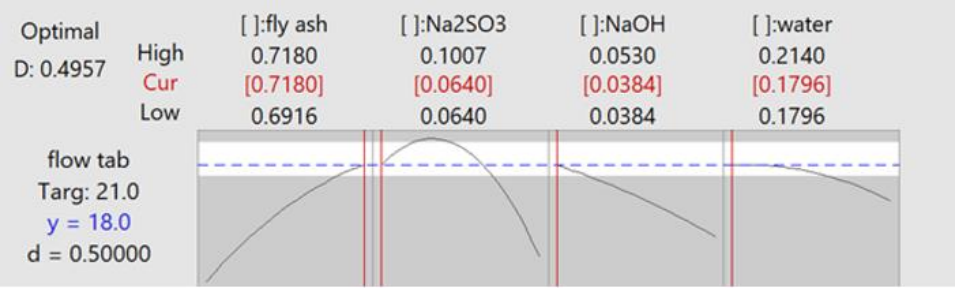

Figure 3.14 Factors affect flow table results for GPM

3.3.2.3. Setting time. Figure 3.15 shows mixtures No.1, No.5, and No.9 had the longest setting times. All the other mixtures had relatively short setting times. Setting time is largely dependent on Na_2SiO_3/ NaOH ratios. Saloma et al. (2017) reported that the lower Na_2SiO_3 and NaOH ratios caused faster setting times, which correlate well with the result of this study. Figure 3.16 shows how each factor affected the setting times. The ratio of Na_2SiO_3 and NaOH played an essential role in influencing the setting time.

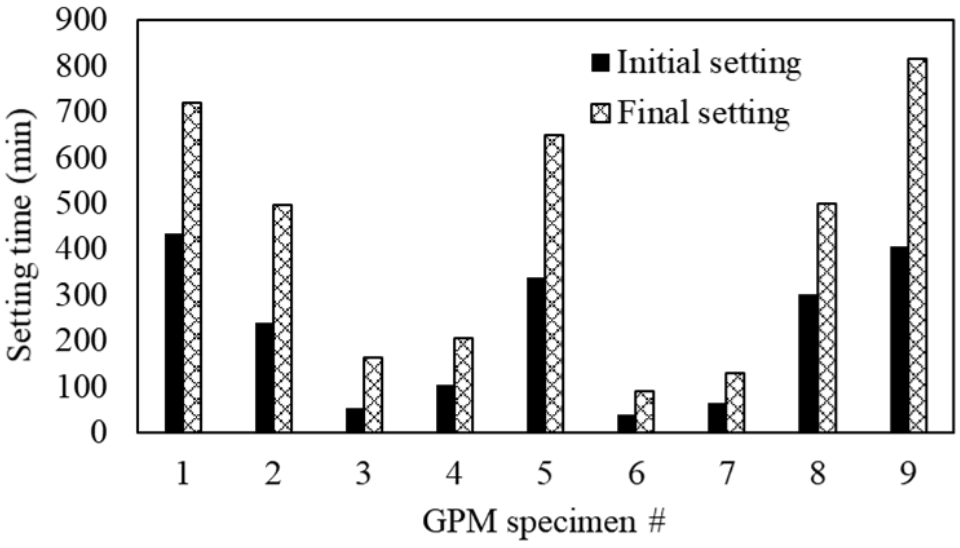

Figure 3.15 Initial and final setting time of each screening mixture for GPM.

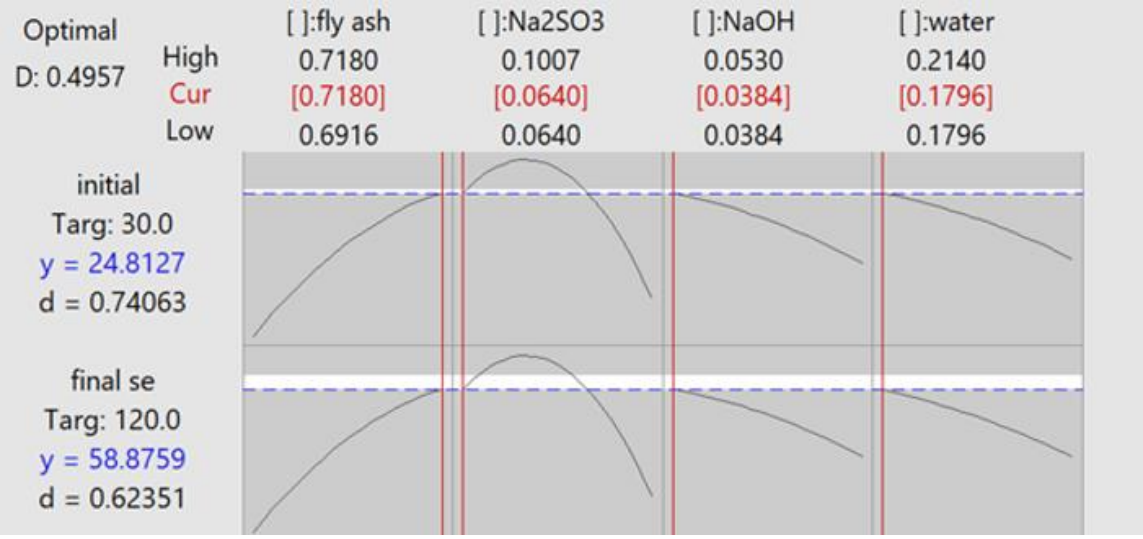

Figure 3.16 Factors affect setting time results for GPM.

3.3.3. MPCM. The results of compressive strength, workability, and setting time for the 9 mixtures of HPCM were discussed in this part, the compressive strength was conducted at 1hour, 2 hours and 24 hours.

3.3.3.1. Compressive strength. For all of the mixtures in Figure 3.17, the 1-hr strengths were nearly the same between 1.4 to 3.4 MPa. Rapid development of the compressive strength was achieved within the second hour. The 2-hr compressive strengths approximately doubled or tripled compared with the 1-hr compressive strengths, and 24-hr compressive strengths were about two to three times those found after 2 hrs, indicating the compressive strength increased slower as time increased. Figure 3.18 is the result from Minitab, which shows that water and borax content was the dominant factor in compressive strength. As water and borax content increased, the compressive strength decreased**.**

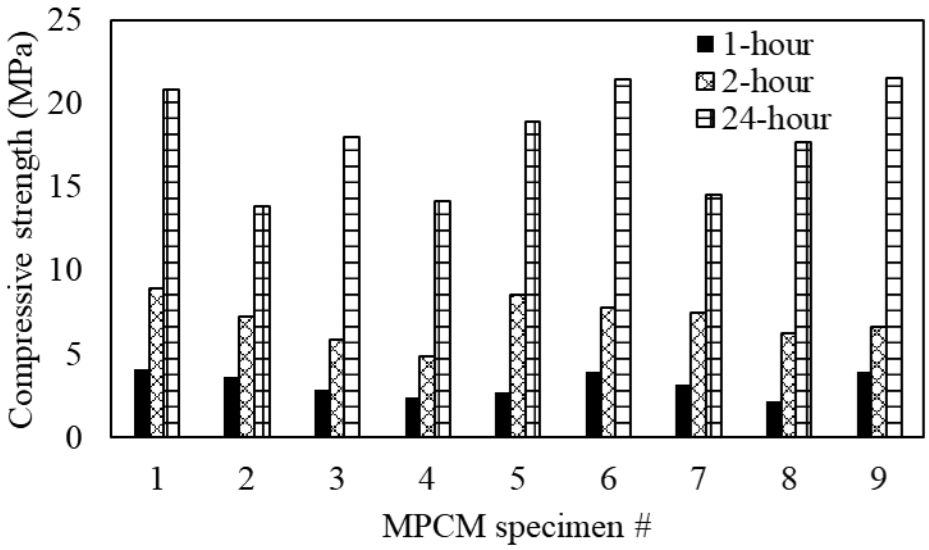

Figure 3.17 Compressive strength at 1, 2, and 24 hours curing of each mixture for MPCM.

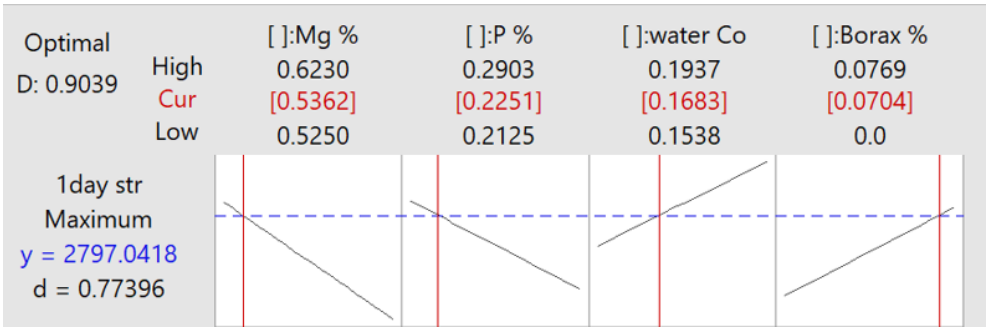

Figure 3.18 Factors affect compressive strength results for MPCM.

3.3.3.2. Workability. Figure 3.19 shows the flow table results, which represent the workability of this mortar. Most of them were within 140 to 210 mm. Figure 3.20 shows that borax content was the dominant factor in flow table results, which means the workability of MPCM was also related to setting time.

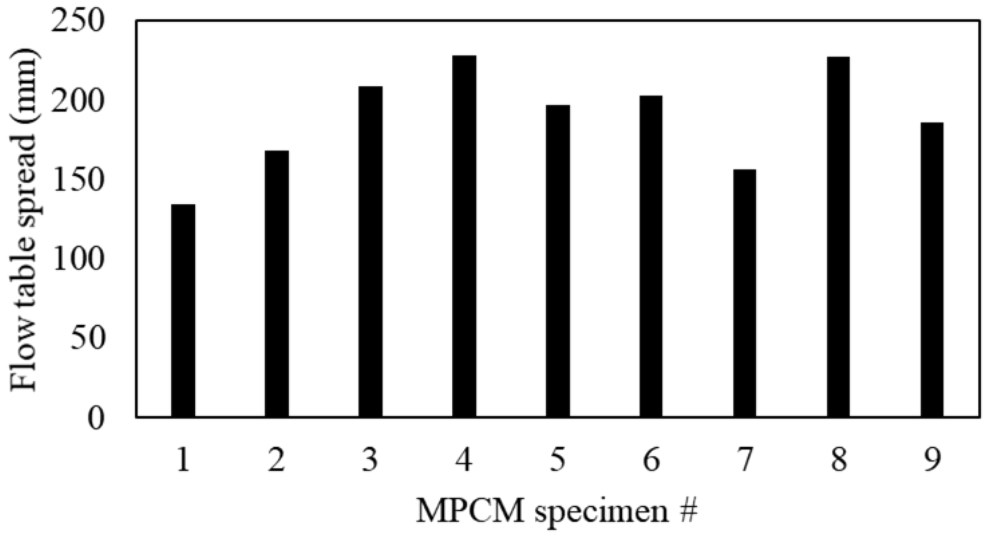

Figure 3.19 Flow table spread result of each screening mixture for MPCM.

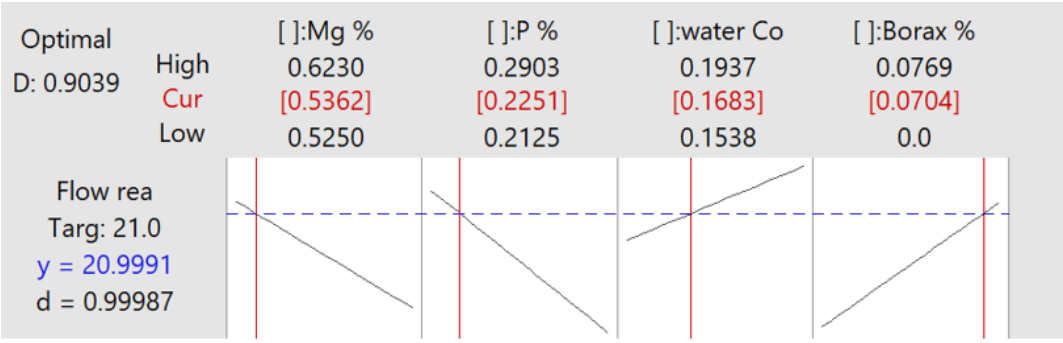

Figure 3.20 Factors affect flow table results for MPCM.

3.3.3.3. Setting time. The initial and final setting times of each mixture are shown in Figure 3.21. Figure 3.21 shows mixtures No.8 and 9 had long setting times. By contrast, No.8 and No.9 had the highest M/P ratios. As shown in Figure 3.22, an increasing M/P ratio resulted in rising final setting time, but it did not affect much of the initial setting. Water content didn't play an essential role in setting time. Increasing borax content could lead the initial and final setting times to significantly increase.

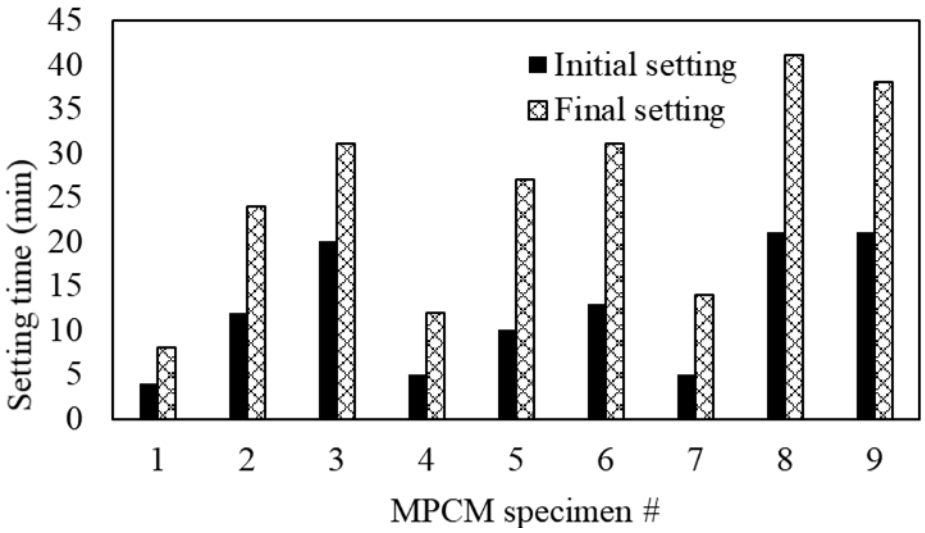

Figure 3.21 Initial and final setting time of each screening mixture for MPCM

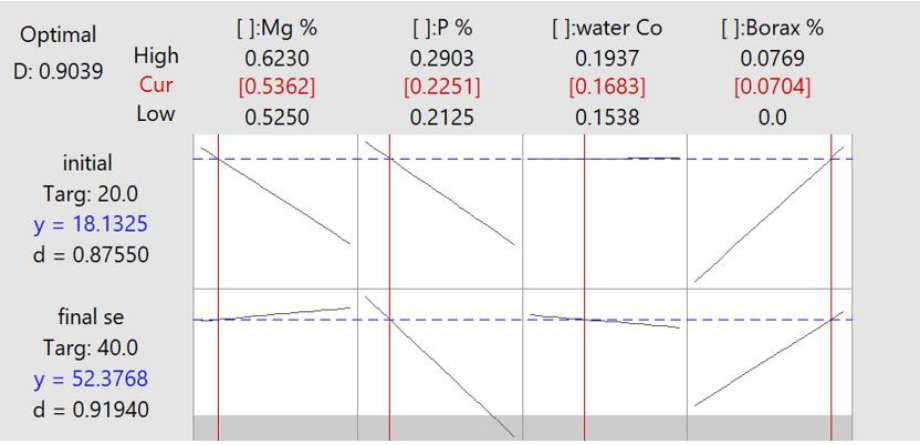

Figure 3.22 Factors affect setting time results for MPCM

3.4. DETERMINING THE OPTIMUM MIXTURE

In the previous section, the optimum formulation was discussed for each test individually. The optimum composition values for each test were not essentially optimum for another test. Therefore, to simultaneously fit all the tests, all variables should be considered. Minitab was used to determine optimum mixture design.

3.4.1. HPCM. Responses included 1, 3, and 7-day compressive strengths, flow readings, initial setting times, and final setting times. The linear models were used to describe how each component affected the response.

Response = A (cement) +B (water) +C (superplasticizer) +D (accelerator) +E (VMA)

After setting the linear model, targets were used to maximize each response. Targets were set approximately 10% higher than the highest average mix measurements, so it improved the reliability to better represent the highest value measured in the lab. For example, mix No. 2 had the highest average 1-day compressive strength. Therefore, 110% of its compressive strength was used as the target. The lower limit was the lowest average measurement. Each response, except flow reading, was set to maximize at these targets. Flow reading was set a range of 150 mm to 230 mm, and the target was set at 200 mm. The upper limit, target, lower limit, weight, and importance for each response were summarized in Table 3.9.

All factors including water, superplasticizer, accelerator, and VMA contents had some effect on all properties of fresh mortar. Since the linear relationship was set in the program, this relationship simplify that all the factors had either a positive or negative linear effect on compressive strengths, flow table readings, and setting times.

As discussed in the previous section, water content had a major effect on compressive strength. As it increased, the compressive strength decreased. High water content also caused early setting. Superplasticizer or water reducer doesn't have much effect on compressive strength and setting times. For flow table reading, the higher the

water reducer content, the higher the flow table reading would be. Accelerator contributed to the fast setting. VMA made the compressive strength lower.

Table 3.9 Responses optimization parameters of HPCM.

Response	Goal	Lower limit	Upper limit	Target	Weight	Importance
Flow table spread	Target	170	230	200	1	2
Initial setting	Minimum	0	400	0	1	2
Final setting	Minimum	0	600	0	1	2
1-day compressive	Maximize	34.47	68.95	68.95	1	2
3-day compressive	Maximize	37.92	75.84	75.84	1	1
7-day compressive	Maximize	41.37	82.74	82.74	1	1

As shown in Table 3.9, all responses were weighed at 1.0, but the important factor, k, was varied. 3-day strength and 7-day strengths were considered of equal importance at 1.0. The important factor of flow reading, the initial setting, the final setting, and 1-day strength were all set at 2.0. The initial setting was the parameter and reflected how well the coating adhered in early stages. Using all these inputs and limits, Minitab determined the optimum mix design to be:

Cement: sand: fly ash: silica fume: water: superplasticizer: accelerator: VMA = 1: 2: 0.15: 0.1: 0.36: 0.012: 0.04: 0.17 (by weight)

The weight of superplasticizer, accelerator, and VMA are bulk weights. The weights of water were the total weight of water needed subtracted by the water contained in superplasticizer, accelerator, and VMA.

Furthermore, the predicted flow readings, initial settings, final settings, and 1, 3, 7-day strength values were based on the mathematical relations, the detailed information is shown in Table 3.10.

Table 3.10 Predicted responses of optimum HPCM mixture.

Response	Predicted results	Desirability
Flow table spread	200.00 mm	0.999091
Initial setting	212.37 min	0.469085
Final setting	264.80 min	0.558671
1-day strength	43.14 MPa	0.651325
3-day strength	51.44 MPa	0.756494
7-day strength	57.11 MPa	0.780714

To validate the predicted results for the optimum formulation of the HPCM in the previous section, more specimens were fabricated and tested under the compressive strength tests, setting time, and flow table tests. The predicted and averaged measured strengths were correlated very well. The flow table test result was 16cm, which indicated that this mixture did not have good workability. Other tests such as setting time and compressive strength showed approximately the same results from the Minitab simulation. The optimum mix design used was:

Cement: sand: fly ash: silica fume: water: superplasticizer: accelerator: VMA = 1: 2: 0.15: 0.1: 0.365: 0.015: 0.04: 0.17 (by weight)

3.4.2. GPM. Minitab was used to determine optimum water/fly ash, fly ash/alkaline activator solution, and Na_2SiO_3/ NaOH ratios. The mix design of optimum

portions of admixtures that affected the flow table readings, compressive strengths, and setting times.

Responses included 1, 3, and 7-day compressive strengths, flow readings, initial setting times, and final settings. The linear models were investigated. Linear models described how each component affected the response.

Response = A (fly ash) +B (water) +C (Na_2SiO_3) +D (NaOH)

After setting the linear model, targets were used to maximize each response. The lower limit was the lowest average measurement. Each response, except flow reading, was set to maximize at these targets. Flow reading was set within the range of 150 mm to 240 mm, and the target was set at 210 mm. The upper limits, target, lower limits, weights, and importance of each response are summarized in Table 3.11.

Using all inputs and limits, Minitab determined the optimum mix design to be:

Fly ash: sand: water: Na_2SiO_3: NaOH = 1: 2: 0.089: 0.0534: 0.250 (by weight)

Furthermore, the predicted compressive strengths, flow readings, initial settings, and final setting time values were based on mathematical relations, as shown in Table 3.12.

To validate the predicted results for the optimum formulation of the GPM mortar in the previous section, more specimens were fabricated and tested under the compressive strengths, setting times, and flow table tests. The predicted results in Table 3.12 and the average measured strengths were correlated very well. The optimum mix design finally adopted was:

Fly ash: sand: water: Na_2SiO_3: NaOH = 1: 2: 0.089: 0.0534: 0.250 (by weight)

Table 3.11 Response optimization of GPM.

Response	Goal	Lower limit	Upper limit	Target	Weight	Importance
Flow table spread	Target	150	240	210	1	2
Initial setting	Minimum	0	400	30	1	2
Final setting	Minimum	0	600	120	1	2
1-day compressive	Maximize	0.69	20.68	20.68	1	2
3-day compressive	Maximize	2.07	20.68	20.68	1	1
7-day compressive	Maximize	4.13	20.68	20.68	1	1

Table 3.12 Predicted responses of optimum GPM mixture.

Response	Predicted results	Desirability
Flow table spread	180.00 mm	0.500000
Initial setting	24.813 min	0.740633
Final setting	58.876 min	0.623506
1-day strength	6.55 MPa	0.693333
3-day strength	13.75 MPa	0.755384
7-day strength	19.07 MPa	0.680671

3.4.3. MPCM. To determine the optimum magnesium/phosphate ratio, water amounts, and borax content, Minitab was used. Responses included 1, 2, and 24-hour compressive strengths, flow table spread, initial setting times, and final setting times. The linear models were investigated. Linear models described how each component affected the response.

Response = A (magnesium) +B (phosphate) +C (water) +D (borax).

The upper limits, targets, lower limits, weights, and the importance of each response are summarized in Table 3.13.

Using all these inputs and limits, Minitab determined the optimum mix design to be:

Magnesium: phosphate: sand: water: borax= 1: 0.420: 2.839: 0.313: 0.132 (by weight)

Table 3.13 Response optimization of MPCM.

Response	Goal	Lower limit	Upper limit	Target	Weight	Importance
Flow table spread	Target	140	240	210	1	1
Initial setting	Minimum	5	60	20	1	1
Final setting	Minimum	20	120	40	0.5	0.5
1-hr compressive	Maximize	0.69	13.79	13.79	0.5	0.5
2-hr compressive	Maximize	3.45	27.58	27.58	0.5	0.5
24-hr compressive	Maximize	6.89	68.95	68.95	0.5	0.5

Furthermore, the predicted 1, 2, and 24-hour compressive strengths, flow readings, initial settings, and final setting time values were based on the mathematical relations, as shown in Table 3.14.

Like HPCM and GPM, the verification was done for MPCM. After some trials, the optimum mix design was eventually determined to be:

Magnesium: phosphate: sand: water: borax= 1: 0.4158: 2.832: 0.324: 0.132 (by weight).

Table 3.14 Predicted responses of optimum MPCM mixture.

Response	Predicted results	Desirability
Flow table spread	210 mm	0.999870
Initial setting	18.13 min	0.875499
Final setting	52.38 min	0.919396
1-hr strength	2.97 MPa	0.613853
2-hr strength	7.11 MPa	0.732954
24-hr strength	19.28 MPa	0.773960

4. PERFORMANCE TESTS of HPCM, GPM and MPCM

Based on the optimum mix designs of HPCM, GPM, and MPCM, the workability, setting time, early-age compressive strength, slip resistance, cohesiveness, and adhesiveness tests were conducted to investigate the feasibility of HPCM, GPM, and MPCM as coating materials. Workability was determined by the flow table test. Together with setting time test and early-age strength, they were conducted using the same procedures as section 3. Slip resistance, cohesiveness, and adhesiveness were evaluated using a novel test method, which was inspired by shotcrete. By checking the mortar status after shooting on a wood pad surface, parameters such as rebound ratio, spray area expansion ratio, and build-up thickness were used to evaluate the slip resistance, cohesiveness, and adhesiveness of the mortar on the vertical wood pad surface. All the properties should meet the construction requirements. Lastly, the fire-resistant performance of the suitable coating materials was investigated using furnace and compared.

4.1. WORKABILITY AND STRENGTH

The workability test evaluated the capability of the fresh mortar to flow. A range of 170 mm to 220 mm was applied as qualified flow table results for fresh mortars. The mortars with a reading less than 170 mm tend to have poor workability, and higher than 220 mm tend to be too flowable. As is shown in Figure 4.1a, all the mortars met this requirement.

Figure 4.1b presents the setting time results of three potential coating materials. It is observed that GPM and MPCM set much faster than HPCM. Based on the analysis of

Minitab's initial screening test, it is concluded that the setting time for GPM was mostly dependent on Na_2SiO_3/NaOH ratios. Lower usage of the Na_2SiO_3/NaOH ratio causes a faster setting time. For MPCM, an increase in the magnesium/phosphate ratio results in an increase in the setting time, and increasing borax increases the setting time. Even with adding borax, MPCM still had faster setting than HPCM and GPM. There's no requirement for initial setting time. The national standards suggest that the final setting time should not be later than 6.5 h. Therefore, the setting time of all materials met construction requirements.

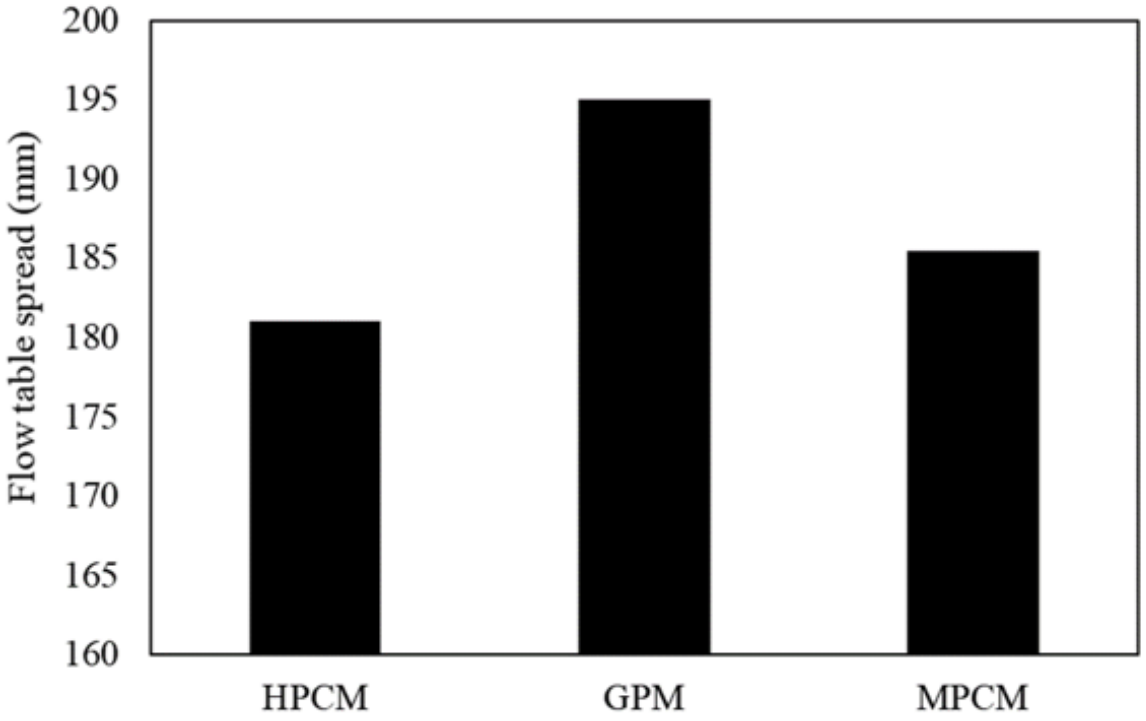

(a)

Figure 4.1 Materials Properties. (a) Flow table, (b) setting time, (c) early-age compressive strength

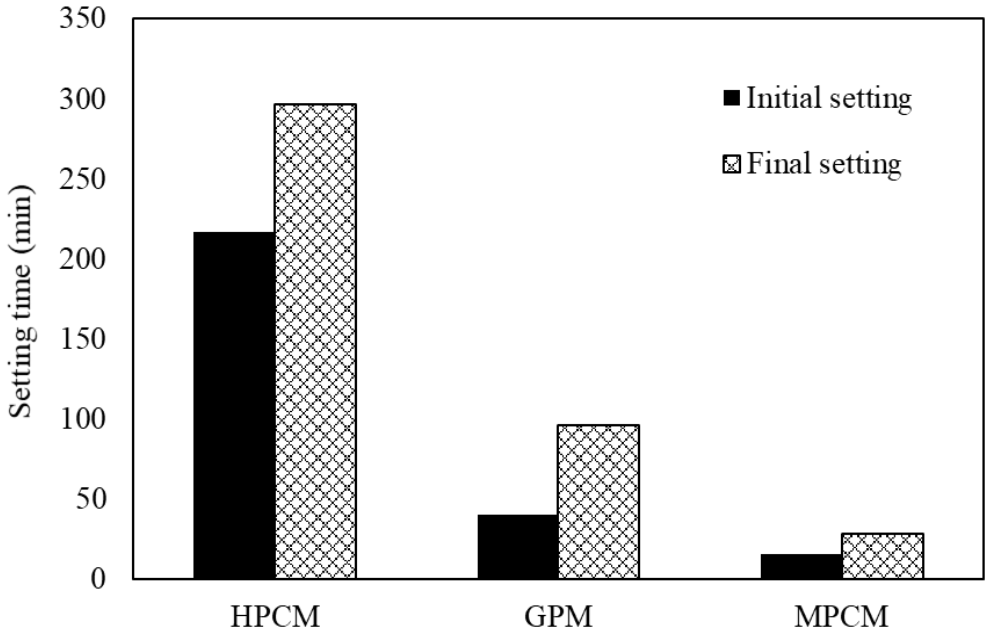

(b)

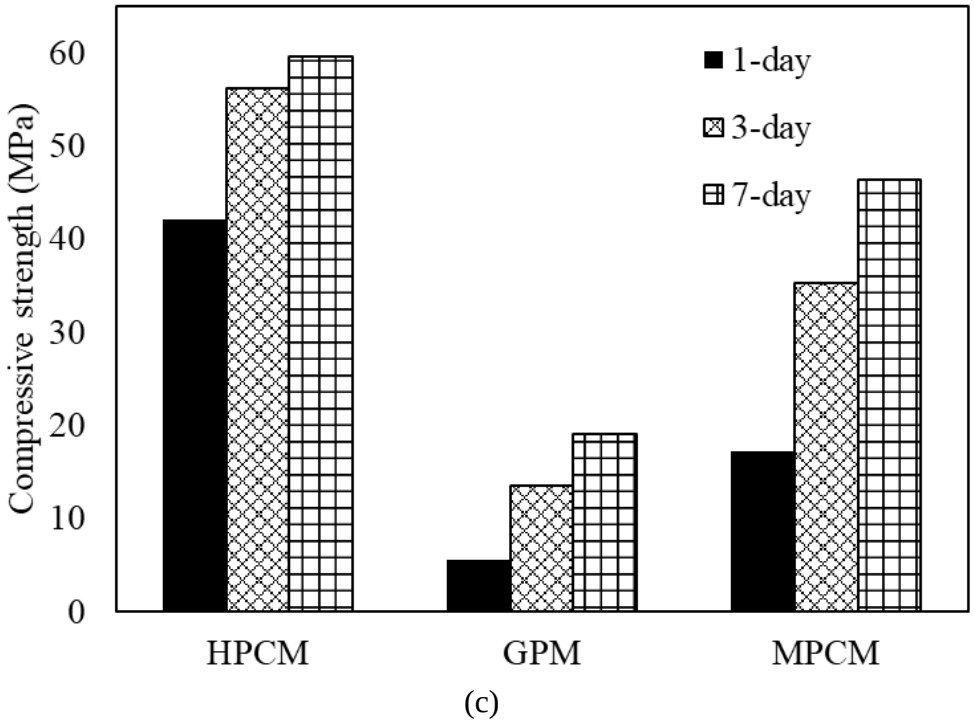

(c)

Figure 4.1 Materials Properties. (a) Flow table, (b) setting time, (c) early-age compressive strength. (cont.)

Figure 4.1c shows the 1-day, 3-day, and 7-day compressive strengths. HPCM had the highest compressive strength, followed by MPCM, and GPM had the lowest compressive strength. As these three materials are designed for coating materials that will not bear any load, ASTM C1328 / C1328M – 19 standard specification for plastic (stucco) cement was followed, suggesting a requirement of 1,300 psi (8.96 MPa) for stucco as a coating material. In this study, by comparing their 7-day compressive strength to the required compressive strength of 8.96 MPa, all these three materials met this requirement.

4.2. SLIP RESISTANCE, COHESIVENESS AND ADHESIVENESS

As coating materials, the mortars should have excellent slip resistance, cohesiveness, and adhesiveness when applying to structures' surface. In this study, the spray method was used to evaluate these parameters. This idea was inspired by shotcrete. In the shotcrete process, the mortar or concrete is projected at a very high speed, and then, the shotcrete will change from a fluid to a sticky material (Lootens et al., 2008). It needs to quickly gain enough strength to be able to build up a respectable layer of sprayed concrete, typically 200–400 mm, in about one hour. More importantly, its strength must continue to increase, typically throughout a couple of hours (Eberhardt et al., 2009). It is widely applied in repair/reinforcement of building elements, rock consolidation, and for the construction of temporary or permanent tunnel linings. A spray test was conducted to test each material's feasibility as a medium of shotcrete. A sprayer shooting set-up (Figure 4.2) was built.

As shown in Figure 4.2, the fresh mortar was poured into a compressed air sprayer and the sprayer and sprayed to the surface of a wood pad vertically placed. In this test, the mortar was sprayed about half of the wood surface area from left to right. A camera was set to record the whole spraying process continuously. Slip resistance was measured using the sprayed mortar area change on the wood. Cohesiveness was measured using the sprayed mortar's build-up thickness. Adhesiveness was measured using its rebound.

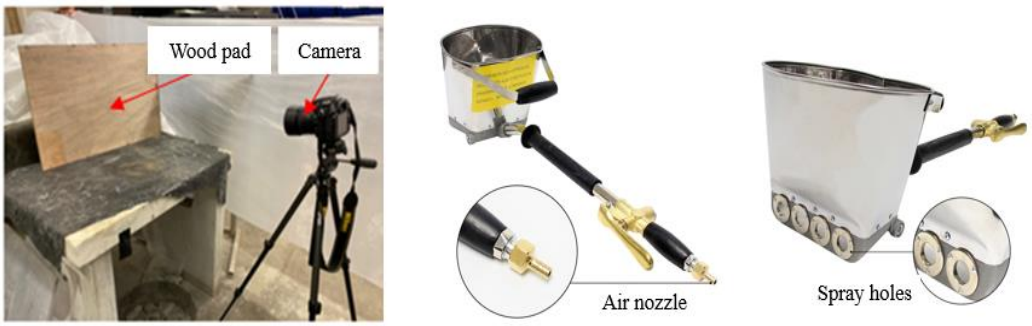

Figure 4.2 Equipment set up for evaluation of slip resistance, cohesiveness, and adhesiveness.

The image processing technology was used to determine the slip resistance of the coating materials by Matlab. The sprayed mortar area on the wood pad can be accurately recorded by the camera and identified by a series of Matlab algorithms. Figure 4.3a presents the image processing procedures. The first step is to identify and project the sprayed mortar area onto a black background. The second step is to convert the sprayed mortar area into a white area. By making the sprayed mortar area in white, the software can recognize it and calculate the white area's total number of pixels.

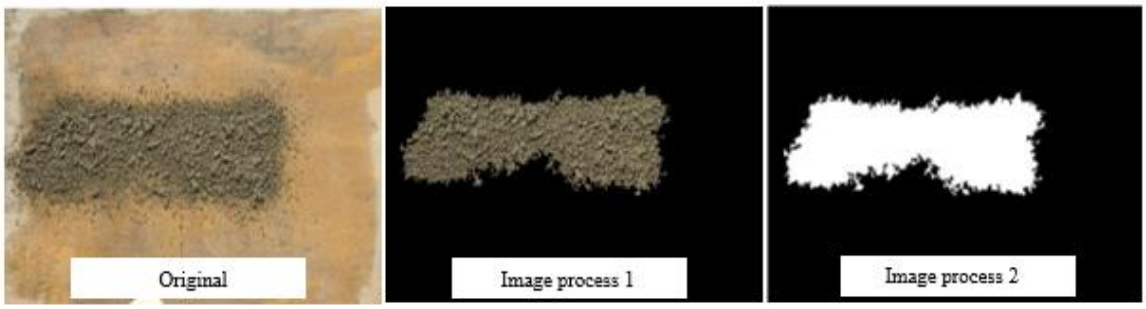

(a)

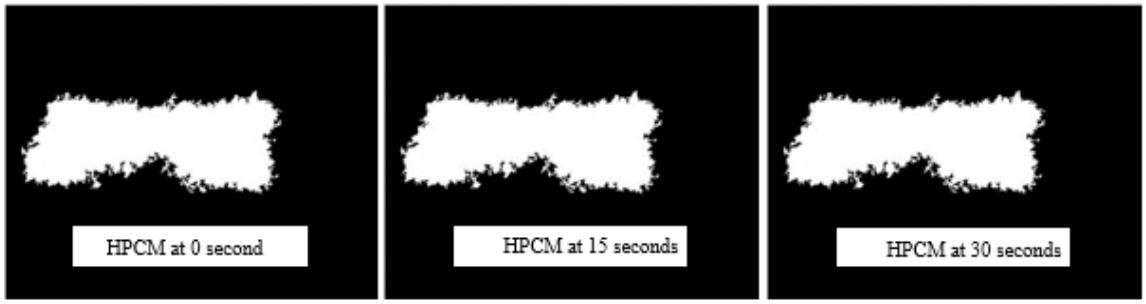

(b)

(c)

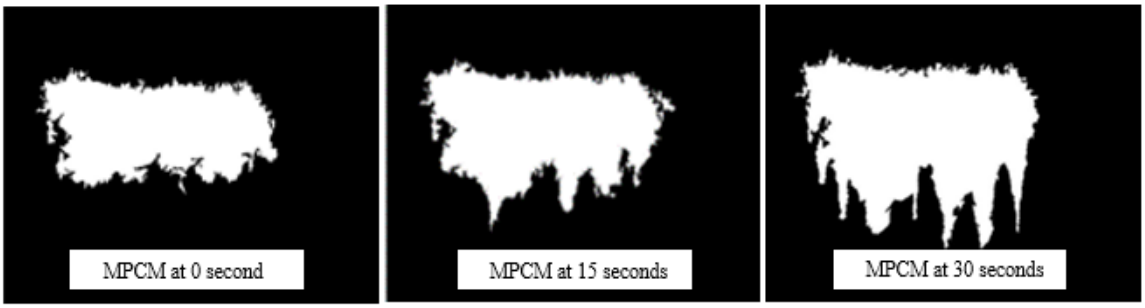

(d)

Figure 4.3 Spray property. (a) image process example using Matlab, (b) HPCM spray areas, (c) GPM spray areas, (d) MPCM spray areas, (e) spray area expansion ratios, (f) build-up thickness, (g) rebound.

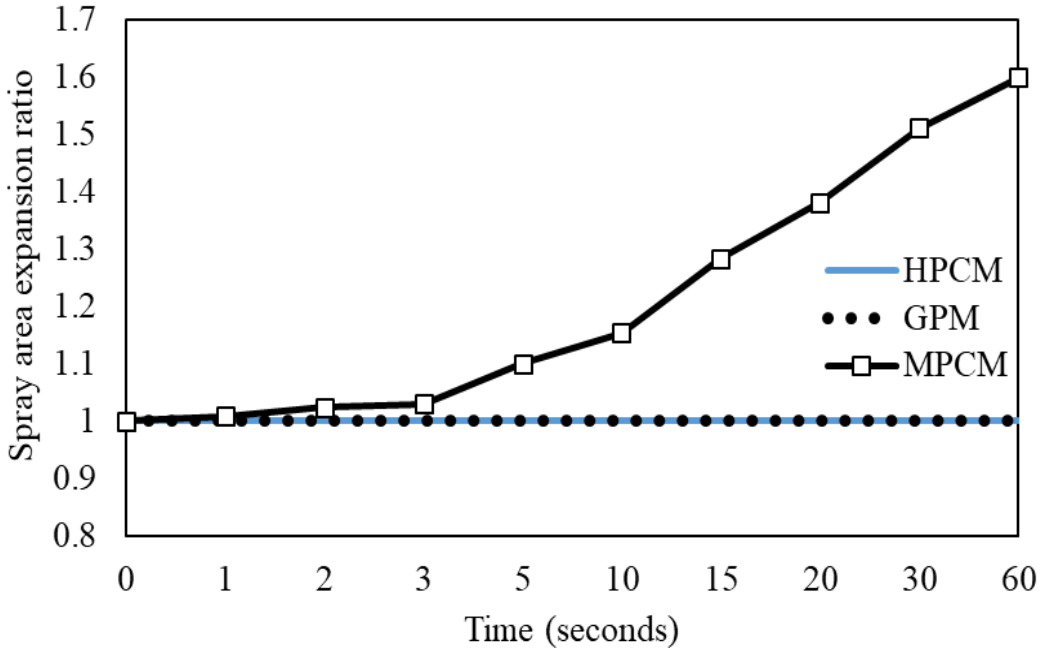

(e)

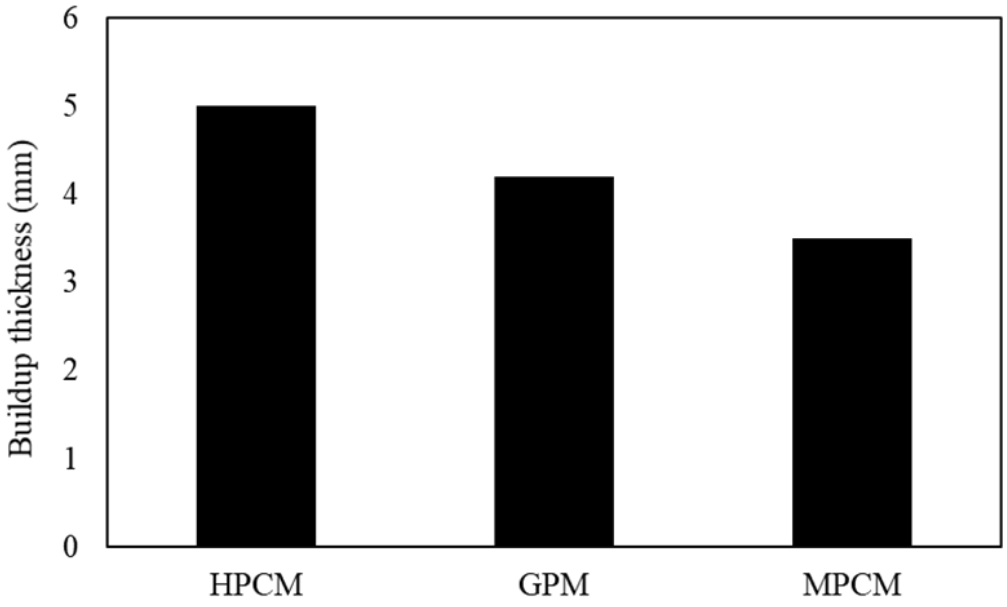

(f)

Figure 4.3 Spray property. (a) image process example using Matlab, (b) HPCM spray areas, (c) GPM spray areas, (d) MPCM spray areas, (e) spray area expansion ratios, (f) build-up thickness, (g) rebound. (cont.)

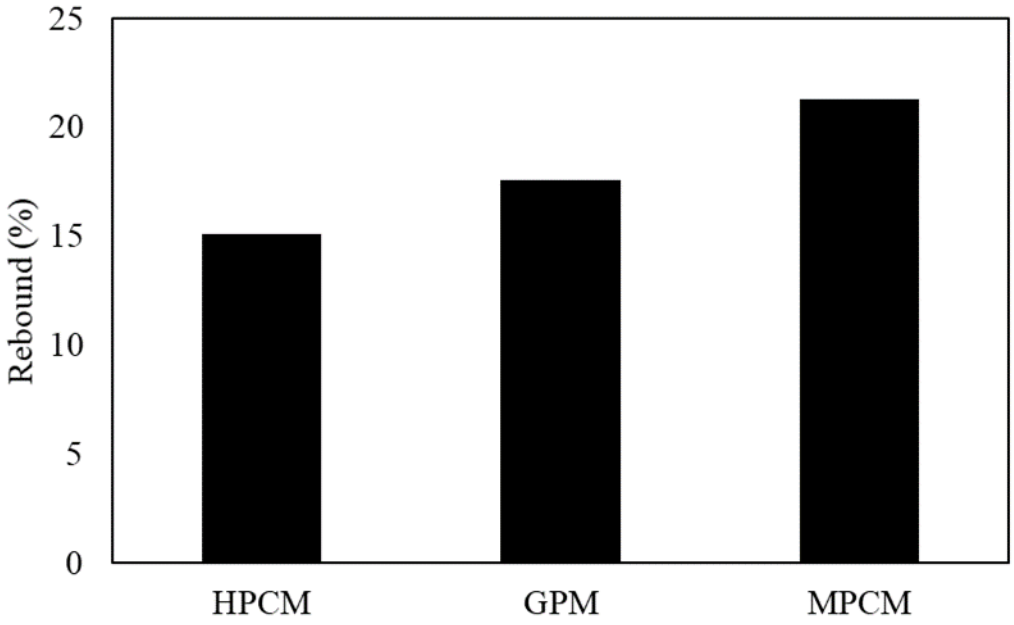

(g)

Figure 4.3 Spray property. (a) image process example using Matlab, (b) HPCM spray areas, (c) GPM spray areas, (d) MPCM spray areas, (e) spray area expansion ratios, (f) build-up thickness, (g) rebound. (cont.)

Figure 4.3b shows the pictures of the HPCM sprayed area at different times after the image processing. Similarly, Figures 4.3c and 4.4d represent the GPM, and MPCM sprayed area pictures at different times after the image processing, respectively. The wood's mortared area was calculated at different times and compared with the initial area (its area at 0 seconds). The increase in area is expressed as a ratio to the initial area. The higher the value, the worse is the slip resistance of the mortar. As is shown in Figure 4.3e, the area expansion ratio grows over time. The higher the slope, the faster the area changes, and the less the slip resistance is. HPCM and GPM had a constant spray area expansion ratio of 1, which means they stuck to the wood pad firmly and didn't slip at all. The requirement for this measurement is less than 2 at 60 seconds. MPCM slipped after

spraying onto the wood plate, but the rate change was still below 2. So all these materials met the workability requirement.

Build-up thickness is an important parameter to estimate the cohesiveness of mortar. It is defined as the maximum thickness that can be a build-up in a stable way (Lukas et al. 1995). Greater build-up thickness indicates better cohesiveness. To measure and compare different materials' build-up thickness, the volume of each fresh mortar retained on the wood pad was measured. The thickness was obtained by dividing retained weight on the wood pad using spray area on the wood pad. The area is also obtained by using Matlab image process. Since the whole area of the wood pad is known, the sprayed area can be obtained by comparing the numbers of sprayed area's pixels at 60 seconds and the number of pixels of the whole wood pad in the picture. Dividing this retained volume by the area calculated, the buildup thickness of each material retain on the wood pad was obtained. Generally, the thicker the coating is, the better the fire-resistant property is. MPCM had the least build-up thickness, and HPCM had the highest build-up thickness. The requirement for this measurement is the thickness ratio should be greater than 2.5 mm. All these three materials met this requirement.

The rebound is defined as the portion of the sprayed material that does not adhere to the substrate. The rebound is represented as a percentage of the total mass of the mass of shot material. It is one of the significant parameters to estimate the adhesiveness of mortar. The rebound on the floor was collected on plastic sheets. The results can show the performance of each mortar qualitatively. In Figure 4.3d, MPCM had the highest rebound, and HPCM had the lowest rebound, indicating HPCM had the best adhesiveness. There's no specific criteria evaluate it now (Lukas et al., 1995). In this

study, the requirement for this measurement was set no higher than 30%. Therefore, all these three materials met the requirement.

Though these three materials showed different slip resistance performance, cohesiveness, and adhesiveness, they all met the requirement of each measurement as coating materials.

4.3. FIRE RESISTANCE

After curing for seven days, cylinder specimens made with HPCM, GPM, and MPCM were exposed to elevated temperatures in a ventilated furnace to investigate their fire resistance (Figure 4.4). The initial ambient temperature in the laboratory was 20 ℃. The temperature in the furnace increased at a rate of 10℃/min. The temperature was set to rise to 1000 ℃.

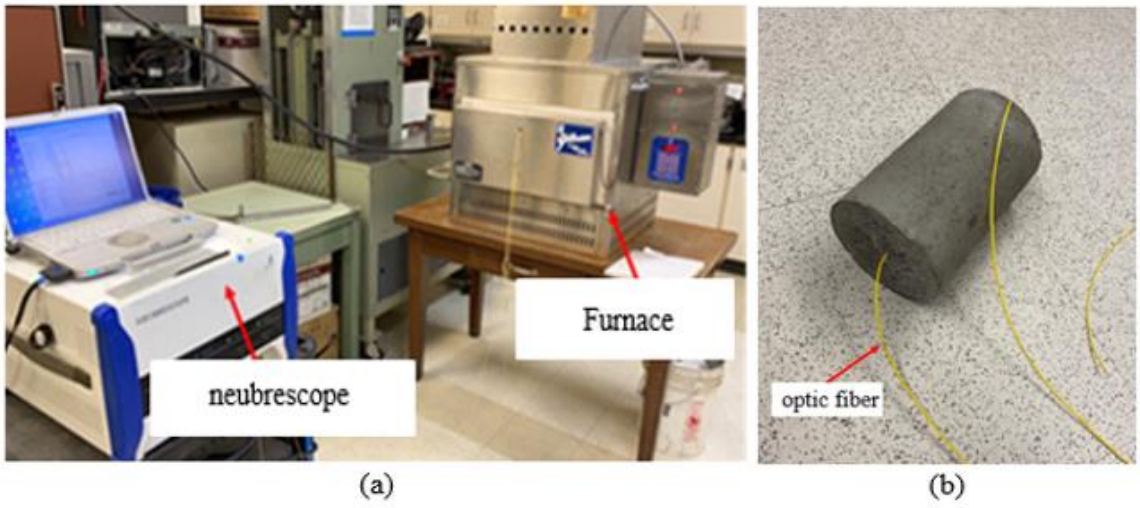

Figure 4.4 Fire resistance test. (a) Equipment, (b) specimens.

The fiber optic sensor was used to monitor the temperature inside specimens. They were cast into the specimens along the centerline. As the specimen was heated in the furnace, the strain distribution along the sensor was measured using the strain and temperature sensing system, Neubrescope. Then, the strain signals were converted to temperatures. The results of elevated temperature monitoring were shown in Figure 4.5a. The temperature was detected at the specimens' centerline, which was the most inside point of the cylinder specimens. By comparing the temperatures at this line at the same time, the heat transfer rate of HPCM, GPM, and MPCM can be determined and compared.

The temperature signals were collected approximately every 5 minutes. At a certain time, the temperature at the center point of the centerline of each specimen can be obtained. As the temperature increased to approximately 650 ℃ at around 65 minutes, the HPCM specimen's signal was lost because of the optic fiber in the cylinder specimen was damaged. The observation in Figure 4.5b shows the HPCM specimen was damaged. So the highest temperature that HPCM can withstand was about 650℃. The signal of a GPM specimen was lost at around 950℃, which means the GPM specimen was broken. The damage of the specimen led to the broken of the optic fiber. The MPCM specimen was heated all the way up to 1000℃ without any damage. Figure 4.5a clearly shows the temperatures in the centers of HPCM, GPM, and MPCM specimens. When the ambient temperature was lower than 650℃, it can be seen that the temperatures at the center of the HPCM were lower than those of GPM and MPCM mortar specimens at a given time. Thus, it takes more time for heat transfer inside HPCM specimen. The slower the temperature increases, the better insulation it is. This means the heat traveled in the

HPCM specimen at a slower rate than in MPCM and GPM specimens. So the HPCM had the best heat insulation property, followed by MPCM and then GPM. When the ambient temperature was higher than 650℃, GPM had slightly better heat insulation than MPCM. By comparing the ambient temperature, MPCM can delay the heat about 30 minutes when ambient temperature was lower than 650℃, GPM can delay the heat about 35minutes, and HPCM can delay the heat about 40 minutes. All of them had similar heat insulation properties, considering the coating in real life is even thinner, different of the insulations of these three materials can be neglected.

Appearance observation, especially cracking and color change, can also help evaluate each material's fire resistance. Figure 4.5b illustrates the HPCM, GPM, and MPCM specimens' surface cracking after exposure to high temperature. From the observation, HPCM had alligator cracking after 650℃ exposure and a very severe spalling problem after 1000℃. GPM and MPCM had better appearance than HPCM at both 650℃ and 1000℃. GPM had a few cracks at 1000℃, while MPCM had none crack, and it mostly looked the same as it was before heating. Obviously, from the observation, MPCM showed the best integrity after heating, followed by GPM, and HPCM had the worst integrity. The color changes of each specimen after high temperature are shown in Figure 4.5b. HPCM specimens did not display much change in color when exposed to high temperatures. The only visible difference was that the grey color became slightly lighter after exposure to high temperatures. This was due to the reduction of moisture in the specimens. There was an obvious color change in GPM after exposure to 650℃ and 1000℃. Before heating, the GPM specimens displayed a very similar surface color as HPCM, but it had changed to a light brown color after 650℃ exposure and brown color

after 1000°C exposure. The GPM samples' color changes were because of the high iron oxide content of the fly ash. A similar color change to brown in fly ash GPMs subjected to high-temperature heat was also observed from another study (Zhao and Sanjayan, 2011). Such color changes are a useful tool for estimating temperatures easily, which have been reached after fire exposure. They can also be used as an indication of significant loss in mechanical properties and are useful since the appearance coincides with a significant reduction in strength due to heating (Short et al., 2001). MPCM didn't show any color change after heating.

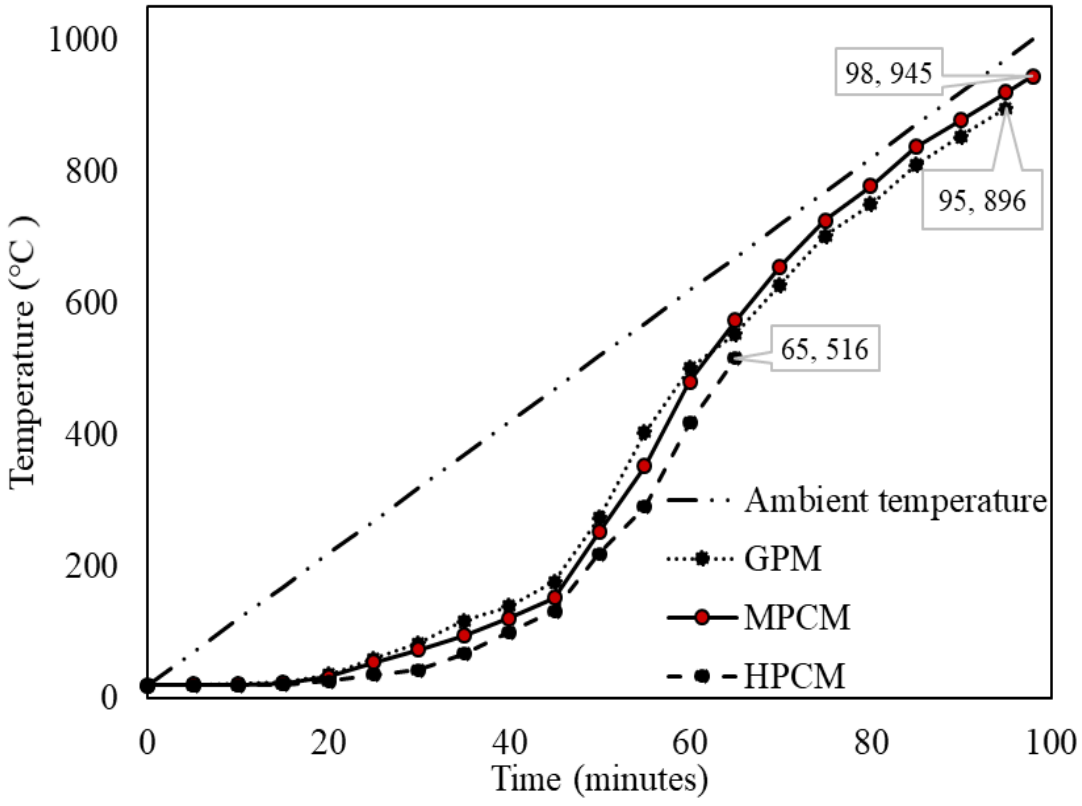

(a)

Figure 4.5 Fire resistance. (a) high-temperature monitoring, (b) representative image of cracking.

(b)

Figure 4.5 Fire resistance. (a) high-temperature monitoring, (b) representative image of cracking. (cont.)

From another study, ordinary Portland concrete showed an average residual strength of 90%, 52%, and 11-16% respectively after exposed to fire at 400℃, 650℃, and 800-1000℃, whereas the average residual strengths of geopolymer concretes were 93%, 82%, and 21-29% after the same treatments. Moreover, the ordinary Portland concrete suffered severe spalling and extensive surface cracking after exposure at 800-1000℃, while there was no spalling and only minor surface cracks in the geopolymer concrete (Zhuang et al., 2016). According to the International Standards Organization standard (ISO 834), Sarker et al. (2014) also tested the fire resistance of the fly ash-based geopolymer concrete and ordinary Portland cement concrete by exposing the samples to fire heating at 400℃, 650℃, 800℃, and 1000℃. When exposed to fire at 1000℃, fly ash-based geopolymer concrete had only minor surface cracking and an average mass loss of only 4.8%. In comparison, ordinary Portland cement concrete had an average mass loss of 90%. There are many factors that influence the spalling of HPCM in high temperature and their interdependency. However, most researchers agree that major causes for fire-induced spalling in concrete are low permeability of concrete and moisture migration in concrete at elevated temperatures (Qiu et al., 2018). During exposure to high temperature, the incredibly high water vapor pressure produced inside the pores of HPCM, when the effective pore pressure go beyond the tensile strength of mortar, lumps of solid mortar fall off. Thus, the lower the porousness of cement, the greater the fire-initiated spalling. Geopolymer had less explosive spalling as a result of the enormous quantities of interconnected little pores inside. The enormous quantities of interconnected little pores increase the escape of moisture when heated, in this way causing less damage to geopolymer mortar (Kong et al., 2007).

There are three relevant concrete failure criteria: (1) Structural adequacy (ability to resist load); (2) Integrity (ability to resist the passage of flames); (3) Insulation (ability to prevent fire spread due to an unacceptable temperature rise of the unheated face) (CCAA, 2010). In this study, mortars are used as coating materials with only 8.96 MPa compressive strength as a minimum requirement for structural adequacy. After heating, observations of pictures indicated that MPCM had the best integrity, followed by a GPM, and HPCM was the worst. It means MPCM had the best ability to resist the passage of flames. For insulation, the temperature vs. times diagram of different materials reveals that HPCM could delay the temperature rising longest when the ambient temperature is less than 650℃, followed by MPCM and GPM. When the temperature was higher than 650℃, HPCM could not serve as insulation anymore because it was broken. When the temperature was higher than 650℃, the GPM had slightly better insulation than MPCM. However, the GPM was broken at 950℃. In reality, the coating is just about 5mm thick, the cracking and spalling issue may be reduced because the temperature differences on both sides may be less than what it is in the cylinder specimens in this study. Also, how each coating material delays the temperature rising would not vary too much. The most important property is if the coating material can isolate the structure from air. Therefore, the coating material's integrity after heating becomes critical. It determines the coating material's best ability to prevent fire spread due to an unacceptable temperature rise. All these three materials passed structural adequacy. MPCM showed the best integrity, followed by a GPM and then HPCM. Overall, when subjected to a high temperature or fire (the fire's temperature is higher than 1000℃), MPCM had the best fire resistance, followed by a GPM and HPCM.

5. CONCLUSION

The objective of this study is to develop mix designs of innovative fire-resistant coating materials including HPCM, GPM, and MPCM, and explore the feasibility of using three types of innovative materials as fire-resistant coating materials for structures. Following this a literature review was done regarding current used fire-resistant material and potential fire-resistant material. In this study, HPCM, GPM, and MPCM mortars were developed as novel fire-resistant coating materials. The workability, early-age strength, and setting time were evaluated in an initial screening using the Taguchi method to determine the mix proportion parameters of HPCM, GPM, and MPCM for coating application. Afterward, the optimum mix design of HPCM, GPM, and MPCM were selected for the further performance tests relevant to fire resistance. The feasibility and potential of these materials as fire-resistant coatings were analyzed and discussed.

Within the scope of this study, HPCM, GPM, and MPCM developed all met construction requirement (compressive strength, workability and setting time). All these three materials had excellent slip resistance, cohesiveness, and adhesiveness as coating materials. HPCM had the highest compressive strength, HPCM and GPM had better slip resistance than MPCM, HPCM and MPCM had better build-up thickness than GPM, and HPCM had the least rebound.

HPCM, GPM, and MPCM can all act as heat insulation to delay the heat transfer into the protected structures. When the ambient temperature is less than 650℃, HPCM had better heat insulation than MPCM and GPM. However, when the ambient temperature was higher than 650℃, HPCM coating could not serve as insulation

anymore because it was broken. It showed alligator cracking at 650℃ and a spalling problem at 1000℃. When the temperature was higher than 650℃, the GPM had slightly better insulation than MPCM. However, the GPM was broken at 950℃, it had a few cracks. When the temperature was higher than 950℃, only MPCM can still serve as an insulation. HPCM and GPM both cracked and broken at this temperature, only MPCM had the integrity.

In reality, the coating is just about 5mm thick, and it serves more as an insulation which isolate the structure from air. How each coating material delays the temperature rising would not vary too much. Therefore, the coating material's integrity after heating is the most important property as an isolation material. It determines the coating material's best ability to prevent fire spread due to an unacceptable temperature rise. MPCM showed the best integrity, followed by a GPM and then HPCM. Overall, when subjected to a high temperature or fire (the fire's temperature is higher than 1000℃), MPCM had the best fire resistance, followed by GPM and HPCM.

Future study will be focused on further refining the mix designs for enhanced fire resistance. Performance of coating materials on various types of structure surfaces will be conducted. The fire resistance of actual structural members coated with the fire-resistant materials on both sides (sandwich specimens) to simulate the real situation will be tested at elevated temperatures. Cost analysis will also be performed to ensure cost effectiveness of mix designs as well.

REFERENCES

Abbas, S. M. L. N., Nehdi, M. L., and Saleem, M. A. (2016). Ultra-high performance concrete: Mechanical performance, durability, sustainability and implementation challenges. *International Journal of Concrete Structures and Materials*, 10(3), 271-295.

ACI. (2012). 234R-06: Guide for the Use of Silica Fume in Concrete. *Technical Documents*. American Concrete Institute. Farmington Hills, MI.

Ali, F. A., O'Connor, D., and Abu-Tair, A. (2001). Explosive spalling of high-strength concrete columns in fire. *Magazine of Concrete Research*, 53(3), 197-204.

Alongi, J., Carosio, F., and Malucelli, G. (2014). Current emerging techniques to impart flame retardancy to fabrics: an overview. *Polymer Degradation and Stability*, 106, 138-149.

Alongi, J., Han, Z., and Bourbigot, S. (2015). Intumescence: tradition versus novelty. A comprehensive review. *Progress in Polymer Science*, 51, 28-73.

Antony, J. and Kaye, M. (2012). Experimental quality: a strategic approach to achieve and improve quality. *Springer Science and Business Media*.

ASCE, Structural Fire Protection. (1992). ASCE Committee on Fire Protection, Structural Division, *American Society of Civil Engineers*, New York, NY, USA.

ASTM International. (2016) C109/C109M-16a Standard Test Method for Compressive Strength of Hydraulic Cement Mortars (Using 2-in. or [50-mm] Cube Specimens). West Conshohocken, PA; *ASTM International*. doi: https://doi.org/10.1520/C0109_C0109M-16A

ASTM International. (2014). C136/C136M-14 Standard Test Method for Sieve Analysis of Fine and Coarse Aggregates. West Conshohocken, PA; *ASTM International*. doi: https://doi.org/10.1520/C0136_C0136M-14

ASTM International. (2014). C230/C230M-14 Standard Specification for Flow Table for Use in Tests of Hydraulic Cement. West Conshohocken, PA; *ASTM International*. doi: https://doi.org/10.1520/C0230_C0230M-14

ASTM International. (2014). C305-14 Standard Practice for Mechanical Mixing of Hydraulic Cement Pastes and Mortars of Plastic Consistency. West Conshohocken, PA; *ASTM International*. doi: https://doi.org/10.1520/C0305-14

ASTM International. (2016). C403/C403M-16 Standard Test Method for Time of Setting of Concrete Mixtures by Penetration Resistance. West Conshohocken, PA; *ASTM International*. doi: https://doi.org/10.1520/C0403_C0403M-16

ASTM International. (2018). C803/C803M-18 Standard Test Method for Penetration Resistance of Hardened Concrete. West Conshohocken, PA; *ASTM International*. doi: https://doi.org/10.1520/C0803_C0803M-18

Brushlinsky, N. N. (2007). Firefighters risks. *Dynamics, management, forecasting. M. FD VNIIPO*.

Crozier, D. A. and Sanjayan, J. G. (1999). Chemical and Physical Degradation of Concrete at Elevated Temperatures. *Concrete in Australia*, 18 - 20.

Davidovits, J. (2002). Environmentally driven geopolymer cement applications. In *Proceedings of 2002 Geopolymer Conference. Melbourne. Australia*.

Dimas, D., Giannopoulou, I., and Panias, D. (2009). Polymerization in sodium silicate solutions: a fundamental process in geopolymerization technology. *Journal of materials science*, 44(14), 3719-3730.

Eberhardt, A. B., Lindlar, B., Stenger, C., and Flatt, R. J. (2009). On the retardation caused by some stabilizers in alkali free accelerators. *In Proceedings of the 17th International Conference on Building Materials*, Weimar.

Evarts, Ben. Fire loss in the United States during 2018. *National Fire Protection Association*, Quincy, MA, 2019. Retrieved from https://www.nfpa.org/~/media/FD0144A044C84FC5BAF90C05C04890B7.ashx

Fang, Y., Cui, P., Ding, Z., and Zhu, J. X. (2018). Properties of a magnesium phosphate cement-based fire-retardant coating containing glass fiber or glass fiber powder. *Construction and Building Materials*, 162, 553-560.

Feng, D., Provis, J. L., and van Deventer, J. S. (2012). Thermal activation of albite for the synthesis of one-part mix geopolymers. *Journal of the American Ceramic Society*, 95(2), 565-572.

Gardner, L. J., Lejeune, V., Corkhill, C. L., Bernal, S. A., Provis, J. L., Stennett, M. C., and Hyatt, N. C. (2015). Evolution of phase assemblage of blended magnesium potassium phosphate cement binders at 200° and 1000° C. *Advances in Applied Ceramics*, 114(7), 386-392.

Giancaspro, J., Balaguru, P. N., and Lyon, R. E. (2006). Use of inorganic polymer to improve the fire response of balsa sandwich structures. *Journal of materials in civil engineering*, 18(3), 390-397.

Grantham, M., Majorana, C., and Salomoni, V. (Eds.). (2009). *Concrete solutions*. CRC Press.

Hall, D. A., Stevens, R., and Jazairi, B. E. (1998). Effect of water content on the structure and mechanical properties of magnesia-phosphate cement mortar. *Journal of the American Ceramic Society*, 81(6), 1550-1556.

He, R., Dai, N., and Wang, Z. (2020). Thermal and Mechanical Properties of Geopolymers Exposed to High Temperature: A Literature Review. *Advances in Civil Engineering*, 2020.

ISO, I. (1999). 834: Fire resistance tests-elements of building construction. *International Organization for Standardization*, Geneva, Switzerland.

Klammert, U., Vorndran, E., Reuther, T., Müller, F. A., Zorn, K., and Gbureck, U. (2010). Low temperature fabrication of magnesium phosphate cement scaffolds by 3D powder printing. *Journal of Materials Science: Materials in Medicine*, 21(11), 2947-2953.

Kodur, V. (2014). Properties of concrete at elevated temperatures. *ISRN Civil engineering*, 2014.

Koksal, F., Gencel, O., Brostow, W., and Lobland, H. H. (2012). Effect of high temperature on mechanical and physical properties of lightweight cement based refractory including expanded vermiculite. *Materials Research Innovations*, 16(1), 7-13.

Kong, D., Sanjayan, J. G., and Sagoe-Crentsil, K. (2007). Comparative performance of geopolymers made with metakaolin and fly ash after exposure to elevated temperatures. *Cement and Concrete Research*, 37, 1583–1589.

Kong, D. L., Sanjayan, J. G. and Sagoe-Crentsil, K. (2008). Factors affecting the performance of metakaolin geopolymers exposed to elevated temperatures. *Journal of Materials Science* 43(3): 824-831

Li, Y., Shi, T., Chen, B., and Li, Y. (2015). Performance of magnesium phosphate cement at elevated temperatures. *Construction and Building Materials*, 91, 126-132.

Lootens, D., Lindlar, B., and Flatt, R. J. (2008). Some peculiar chemistry aspects of shotcrete accelerators. *In Proceedings of the 1st International Conference on Microstructure Related Durability of Cementitious Composites* (pp. 1255-1261).

Lukas, W., Kusterle, W., and Pichler, W. (1995). Innovations in shotcrete technology (No. CONF-9506349-). *American Society of Civil Engineers*, New York, NY.

Lyon, R. E., Balaguru, P. N., Foden, A., Sorathia, U., Davidovits, J., and Davidovics, M. (1997). Fire-resistant aluminosilicate composites. *Fire and materials*, 21(2), 67-73.

McLellan, B. C., Williams, R. P., Lay, J., Van Riessen, A., and Corder, G. D. (2011). Costs and carbon emissions for geopolymer pastes in comparison to ordinary portland cement. *Journal of cleaner production*, 19(9-10), 1080-1090.

Nguyen, K. S., Nguyen, P. V., Nguyen, H., Nguyen, T. N., and Nguyen, T. H. (2012). Use of phosphate magnesium material in fire protection of concrete. *In Proceeding of The 5th ACF Asian Concrete Federation International Conference* (pp. 24-26).

Pan, Z., Sanjayan, J. G. and Rangan, B. V. (2009). An investigation of the mechanisms for strength gain or loss of geopolymer mortar after exposure to elevated temperature. *Journal of Materials Science* 44(7): 1873-1880.

Park, J. W., Kim, K. H., and Ann, K. Y. (2016). Fundamental properties of magnesium phosphate cement mortar for rapid repair of concrete. *Advances in Materials Science and Engineering*, 2016.

Pimraksa, K., Chindaprasirt, P., Rungchet, A., Sagoe-Crentsil, K. and Sato, T. (2011). Lightweight geopolymer made of highly porous siliceous materials with various Na_2O/Al_2O_3 and SiO_2/Al_2O_3 ratios. *Materials Science and Engineering*: A 528(21): 6616-6623.

Qiu, X., Li, Z., Li, X., and Zhang, Z. (2018). Flame retardant coatings prepared using layer by layer assembly: a review. *Chemical Engineering Journal* 334, 108-122.

Ranjit, R. (2001). Design of experiments using the taguchi approach 16 steps to product and process improvement, Inc. *Jony wiley and sons*, 101-103.

Saloma, Hanafiah, Elysandi, D. O., and Meykan, D. G. (2017). Effect of Na_2SiO_3/NaOH on mechanical properties and microstructure of geopolymer mortar using fly ash and rice husk ash as precursor. *In AIP Conference Proceedings* (Vol. 1903, No. 1, p. 050013). AIP Publishing LLC.

Sarker, P. K., Kelly, S., and Yao, Z. (2014). Effect of fire exposure on cracking, spalling and residual strength of fly ash GPM concrete. *Materials and Design*. 63, 584-592.

Seehra, S. S., Gupta, S., and Kumar, S. (1993). Rapid setting magnesium phosphate cement for quick repair of concrete pavements—characterisation and durability aspects. *Cement and Concrete Research*, 23(2), 254-266.

Shaikh, Faiz and Vimonsatit, Sorn. (2014). Compressive strength of fly-ash-based geopolymer concrete at elevated temperatures. *Fire and Materials*. 39. 10.1002/fam.2240.

Short, N. R., Purkiss, J. A., and Guise, S. E. (2001). Assessment of fire damaged concrete using colour image analysis. *Construction and building materials*15(1), 9-15.

Sugama, T. and Kukacka, L. E. (1983). Magnesium monophosphate cements derived from diammonium phosphate solutions. *Cement and concrete research*, 13(3), 407-416.

Tang, F., Chen, G., Volz, J. S., Brow, R. K., and Koenigstein, M. L. (2013). Cement-modified enamel coating for enhanced corrosion resistance of steel reinforcing bars. *Cement and Concrete Composites*, 35(1), 171-180.

Unz, M. (1960). Insulating Properties of Cement Mortar Coating. *Corrosion*, 16(7), 343t-353t.

Vandersall, H. L. (1971). Intumescent coating system, their development and chemistry. *J Fire Flamm*, 2, 97-140.

Van Riessen, A., Rickard, W., and Sanjayan, J. (2009). Thermal properties of geopolymers. *In geopolymers* (pp. 315-342). Woodhead Publishing.

Vickers, L., Van Riessen, A., and Rickard, W. D. (2015). Fire-resistant geopolymers: Role of fibres and fillers to enhance thermal properties. Springer Singapore.

Wilson, A. D. and Nicholson, J. W. (2005). Acid-base cements: their biomedical and industrial applications (Vol. 3). Cambridge University Press.

Yang, N., Shi, C., Yang, J., and Chang, Y. (2014). Research progresses in magnesium phosphate cement–based materials. *Journal of Materials in Civil Engineering*, 26(10), 04014071.

Yunsong, J. (2002). A new type of light magnesium cement foamed material. *Materials Letters*, 56(3), 353-356.

Z. Li, Z. Ding, and Y. Zhang. (2004). Development of sustainable cementitious materials, *Proceedings of International Workshop on Sustainable Development and Concrete Technology*, Beijing, China, pp. 55–76.

Zhang, Y., Wang, Y. C., Bailey, C. G., and Taylor, A. P. (2013). Global modelling of fire protection performance of an intumescent coating under different furnace fire conditions. *Journal of fire sciences*. 31(1), 51-72.

Zhang, Z., Shi, G., Wang, S., Fang, X., and Liu, X. (2013). Thermal energy storage cement mortar containing n-octadecane/expanded graphite composite phase change material. *Renewable Energy*, 50, 670–675. https://doi.org/10.1016/j.renene.2012.08.024

Zhao, R., and Sanjayan, J. G. (2011). GPM and Portland cement concretes in simulated fire. *Magazine of Concrete research*. 63(3), 163-173.

Zhuang, X. Y., Chen, L., Komarneni, S., Zhou, C. H., Tong, D. S., Yang, H. M., and Wang, H. (2016). Fly ash-based GPM: clean production, properties and applications. *Journal of Cleaner Production*. 125, 253-267.

VITA

Anyou Zhu grew up in Changzhou, China. He earned his Bachelor of Science in Civil Engineering from the University of Alaska Fairbanks in Fairbanks, Alaska in May 2018. Later, in December 2020, he earned his Master of Science in Civil Engineering from Missouri University of Science and Technology in Rolla, Missouri.